PALEONTOLOGY

Tracking bioturbation through time: The evolution of the marine sedimentary mixed and transition layers

Lidya G. Tarhan[1]*, Kate H. Pippenger[1], Alison T. Cribb[2], Michelle Zill[3], William Phelps[4], Mary L. Droser[5], David J. Bottjer[3], Matthew E. Clapham[6]

The physical, biogeochemical, and ecological properties of the modern seafloor are extensively shaped by the activities of burrowing and sediment-mixing animals, processes collectively known as bioturbation. Bioturbation is primarily recorded by homogenized sediments of the seafloor mixed layer and the underlying transition layer of discrete burrows. Although these two zones can be readily measured today, there has been limited understanding of how the mixed and transition layers evolved over the Phanerozoic since animals first began to extensively colonize the seafloor. Here, we provide a record for the depths of the sedimentary mixed and transition layers through the Phanerozoic. We find that although deepening of the sediment mixed layer spanned hundreds of millions of years, a deep transition layer was established as early as the Cambrian and did not further deepen until the Mesozoic—trajectories reflecting evolutionary radiations, changes in nutrient cycling, and alleviation of oxygen stress.

INTRODUCTION

Bioturbation is one of the foremost examples of animal-mediated ecosystem engineering across a wide range of environments on Earth's surface. Bioturbating animals substantially affect the rheology, biogeochemistry, and ecology of seafloor sediments, as well as ocean-wide nutrient cycling. Most notable is the formation of a mixed layer of well-churned, biologically homogenized sediments that extends downward from the sediment-water interface to, on average, nearly 10 cm depth in the seafloor, and an underlying transition layer composed of discrete and actively occupied deep burrows that may, in certain settings, extend to >1 m deep (*1*–*3*). Given bioturbators' critical contributions as ecosystem engineers today, the emergence of intensively bioturbated seafloor sediments and both deep and pervasive mixed and transition layers is widely considered to have profoundly affected coeval marine environments and ecosystems (*3*–*5*).

The sedimentary record provides a critical window into the evolutionary development of bioturbation and associated geobiological feedbacks. The trace fossil record of animal-sediment interactions—particularly burrows, trackways and trails—provides snapshots of changes in the ecologies of benthic and infaunal animals through the Phanerozoic. However, the timing and nature of changes in both burrowing depth and, in particular, sediment mixing have historically been much more poorly constrained. In light of the profound engineering impact of bioturbation in modern seafloor sediments, a wide range of biogeochemical, paleobiological, and taphonomic phenomena have nonetheless been attributed to the advent of intensive sediment mixing and deep burrowing (*6*–*8*), largely on the basis of apparent changes in the type and disparity (ichnodiversity and ichnodisparity) of trace fossils. However, neither the morphology of discrete trace fossils nor the ichnotaxonomic composition of trace fossil assemblages is, in isolation, a robust proxy for sediment-mixing intensity, as discrete trace fossils largely record infaunal activity not in the mixed layer but rather in the underlying transition layer (*2*). Although the presence or absence of particular burrowing tiers can help to constrain mixed layer development, these must be combined with sedimentological proxies that can more directly constrain intensities and depths of sediment mixing—particularly characterization of the extent to which sedimentary fabrics are disrupted by bioturbation (ichnofabrics; Fig. 1). However, sediment-mixing intensities and depths may change markedly even on very fine stratigraphic and spatial scales (*4*) and are associated with a wide range of environmental and ecological factors (*3*, *9*). Therefore, these data must be collected systematically and continuously in a detailed stratigraphic and facies-controlled context, from either field exposures or sediment cores, to disentangle secular trends in sediment mixing from paleoenvironmental disparity (*4*, *10*, *11*). Although discrete trace fossils have historically provided key insights into infaunalization (seafloor colonization by burrowing infauna) and variability in tiering depths through time (*12*–*14*), quantitative analyses of large datasets of burrow depth observations have not previously been used to assess, in a statistical framework, patterns in transition layer depth across depositional environments and different intervals of Earth's history.

To unravel the evolution of bioturbation and elucidate to what extent changes in either sediment mixing or burrowing have contributed to the transformation of Earth's surface environments and the nature of the stratigraphic record, we herein reconstruct, from sedimentological and paleontological records, changes in (i) the depth and intensity of sediment mixing and (ii) the depth of the transition layer over the Phanerozoic. We describe existing records and interpretations for the Phanerozoic trajectory of the sedimentary mixed layer, and we present an analysis of burrow depth data to provide updated constraints on the Phanerozoic evolution of the sedimentary transition layer. We additionally highlight intervals for which primary data are currently inadequate. In particular, with limited exception (e.g., the lower Paleozoic, the Permian–Triassic transition, and recent intervals of the Cenozoic), the data necessary to robustly quantify mixed layer depths are sparse to nonexistent, hampering efforts to reconstruct evolutionary, paleoenvironmental, and paleogeographic trends; generating these data should be a key priority for future studies. Nonetheless, those data available—which we review here—yield broad-scale, critical insights into

[1]Department of Earth and Planetary Sciences, Yale University, New Haven, CT 06511, USA. [2]School of Ocean and Earth Science, University of Southampton, Southampton SO17 1BJ, UK. [3]Department of Earth Sciences, University of Southern California, Los Angeles, CA 90089, USA. [4]Department of Geology, Riverside Community College, Riverside, CA 92506, USA. [5]Department of Earth and Planetary Sciences, University of California, Riverside, Riverside, CA 92521, USA. [6]Department of Earth and Planetary Sciences, University of California, Santa Cruz, Santa Cruz, CA 95064, USA.
*Corresponding author. Email: lidya.tarhan@yale.edu

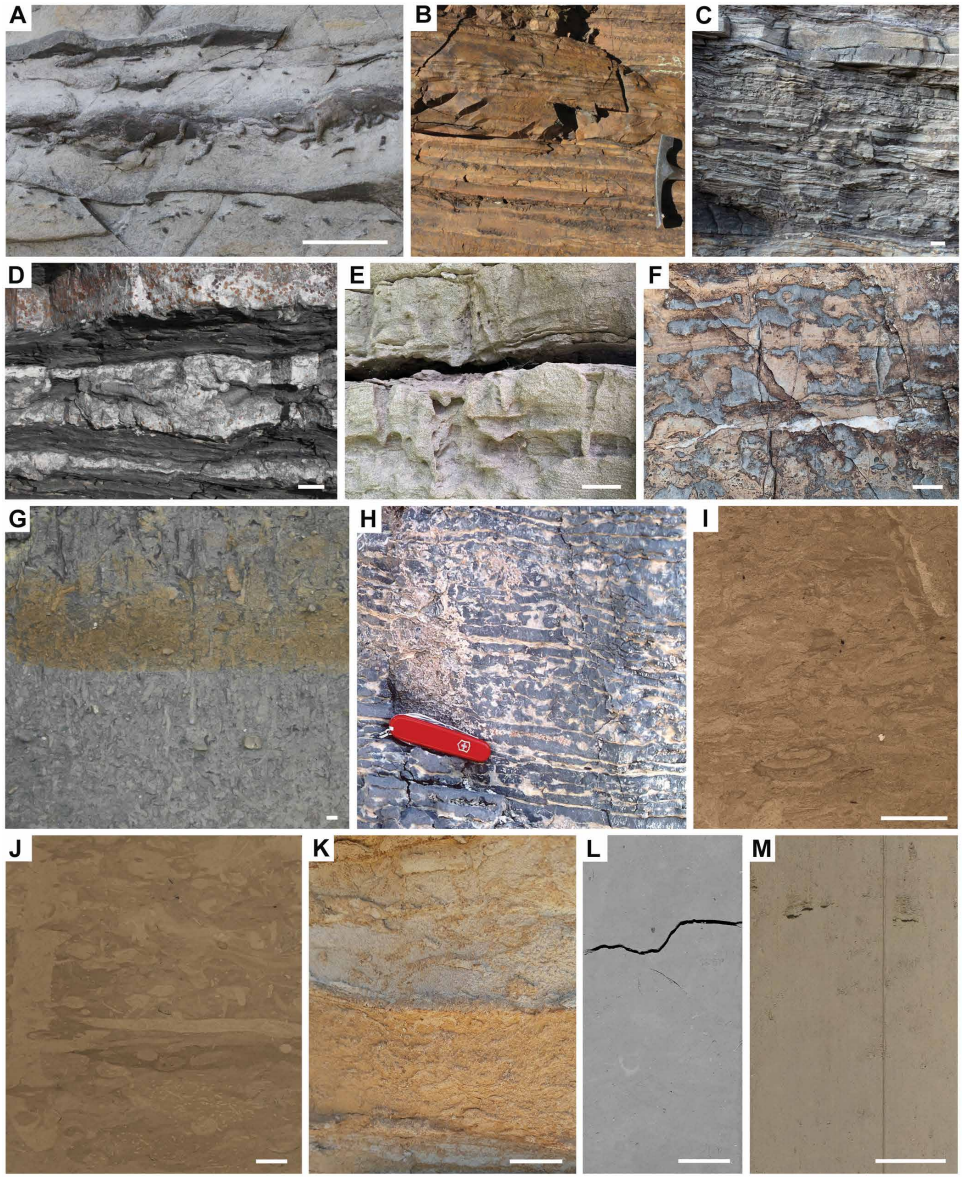

Fig. 1. Characteristic ichnofabrics recording seafloor sediment-mixing intensities through the Phanerozoic. (**A**) Lowermost Cambrian Chapel Island Formation (Newfoundland, Canada), interbedded ii 1 and ii 2, shallow subtidal to inner shelf. (**B**) Lower Cambrian Torréarboles Sandstone (Extremadura, Spain), interbedded ii 1 and ii 2, shoreface to shallow inner shelf. (**C**) Tremadocian to Middle Ordovician Powers Steps Formation (Newfoundland, Canada), interbedded ii 2 and ii 3, storm-dominated nearshore to inner shelf. (**D**) Llandoverian Tuscarora Formation (Pennsylvania, USA), interbedded ii 2, ii 3, and ii 4, estuarine to inner shelf. (**E**) Givetian Moscow Formation (New York, USA), ii 2 to ii 3, shoreface. (**F**) Famennian Guilmette Fm (Nevada, USA), ii 3, inner shelf. (**G**) Kungurian Pebbley Beach Formation (New South Wales, Australia), ii 5, lower shoreface to upper offshore. (**H**) Olenekian Moenkopi Formation (Virgin Limestone Member; Nevada, USA), interbedded ii 1 and ii 4, middle shelf. (**I**) Upper Cretaceous Tropic/Tunuck Shale (Utah, USA), ii 5, lower shoreface to offshore. (**J**) Campanian Demopolis Chalk (Alabama, USA), ii 5, coastal plain shelf. (**K**) Middle Eocene Scripps Formation, ii 5 overlying ii 3, distal deltaic to slope. (**L**) Upper Miocene, ODP site 746 (Southern Ocean), ii 6, deep abyssal. (**M**) Pleistocene, IODP site U1409 (North Atlantic), ii 6, deep abyssal. (A) Modified from (*33*). Scale bars, 2 cm; length of head of hammer in (B) is 17 cm; length of pocket knife in (H) is 8.2 cm.

Phanerozoic mixed layer evolution and suggest both parallels to and notable disparities from concurrent patterns in transition layer evolution. In this review, we focus on shallow marine systems, as these settings experienced many of the earliest (and frequently most dramatic) changes in bioturbation depths, because of the considerable influence of shallow marine systems on ocean-wide biogeochemical cycling, and due to the higher-resolution records provided by shallow marine stratigraphic successions. In addition, we briefly review available (albeit sparser) archives of sediment mixing and deep burrowing in deep-sea settings, as well as bioturbation trends in nearshore settings.

RESULTS

Pre-Phanerozoic records of shallow marine bioturbation

Although rare and simple trace fossils have been reported from middle to lower-upper Ediacaran strata [e.g., ca. 571 to 560 million

years ago (Ma)] (*15*), the oldest relatively abundant and unequivocally bilaterian-produced burrows have been documented in upper Ediacaran strata, commonly in association with White Sea– and Nama-type macrofossil assemblages of the soft-bodied Ediacara Biota (*16*). These burrows (commonly described as *Helminthoidichnites*) consist of curvilinear, leveed structures preserved in both positive and negative relief on the tops and bases of thin, discontinuous sandstone beds (*17*, *18*). This distinctive preservation—particularly intratrace variation between negative and positive relief, and frequent association with microbially mediated sedimentary structures, has led to interpretation of Ediacaran *Helminthoidichnites* as recording the activities of undermat-mining animals (*19*). *Lamonte trevallis*—full-relief burrows associated with microbial sedimentary textures from the upper Ediacaran of South China and the western United States—have likewise been interpreted as structures created by undermat miners (*20*, *21*).

More complex styles of burrowing are recorded in uppermost Ediacaran strata. For instance, small "plug"-type burrows (compare to *Conichnus*) (*22*), as well as treptichnid-type serial chains of isolated or overlapping ridges and knobs (*23*–*25*) have been observed in uppermost Ediacaran strata worldwide. Semi- to shallowly infaunal scribbling, meandering, and spiraling "bulldozing" traces (*Parapsammichnites pretzeliformis*) have also been described from the uppermost Ediacaran Spitskop Member of the Nama Group (*26*). Meiofaunal burrow networks (compare to *Multina minima*) have been documented from the uppermost Ediacaran Corumbá Group of Brazil (*27*). However, these uppermost Ediacaran trace fossils are rare (commonly reported from only a single specimen, bedding plane, or locality), small (typically millimeter scale), and would have been confined to the shallowest region (upper millimeters) of the sediment pile (*24*). On the whole, Ediacaran infaunalization was relatively limited and sediment mixing was nearly nonexistent.

The Phanerozoic evolution of the sediment mixed layer

Early Paleozoic sediment mixing

The first appearance of the index fossil *Treptichnus pedum* and other shallowly penetrative burrows in lowermost Cambrian strata has long been regarded as a marker of major increases in the complexity and extent of seafloor infaunalization (*28*) and changes in seafloor substrate character—particularly the decline of Ediacaran-style matgrounds and emergence of Phanerozoic-style, well-bioturbated mixgrounds (*29*, *30*). Cambrian trace fossil assemblages indicate that infaunal locomotion and burrow construction were well advanced across a range of shallow marine settings by the early Cambrian (*28*, *31*). However, field-based, integrated assessment of sedimentological metrics and preservation of trace fossil assemblages across a range of lower Cambrian facies has indicated that sediment mixing was only poorly to moderately developed during this interval [Materials and Methods and data S1; (*10*, *31*–*33*)]. Lower Cambrian sedimentary fabrics are poorly disrupted. As evaluated using the ichnofabric index (ii) (*34*), in which ii 1 indicates undisrupted depositional stratification and ii 5 indicates complete overprinting of physical stratification by bioturbation, lower Cambrian heterolithic siliciclastic and carbonate strata only rarely exceed ii 3 and are most commonly characterized by ii 1 or 2 (*4*). Lower Cambrian sandstone tempestites are, on average, thinly bedded relative to younger stratigraphic successions [e.g., a recent study (*35*) reported a mean sandstone bed thickness of 1.3 cm from heterolithic successions recording a range of shallow marine settings]. In modern seafloor settings, bioturbators commonly mix sediments across bed junctions, blending adjacent bedforms and thus "erasing" the thinnest beds (*36*). The presence of extremely thin sandstone event beds in lower Cambrian successions therefore indicates limited inter-bed homogenization by coeval bioturbators [data S1; (*4*, *36*)]. Meiofauna-scale and millimeter-scale burrows are common whereas large and deep fabric-disruptive burrowing is uncommon in these deposits (*31*, *33*). Surficially produced and shallow-tier trace fossils and abiogenic sedimentary structures (e.g., tool marks) are remarkably common and exceptionally preserved in lower Cambrian strata, testifying to the cohesive and poorly mixed nature of seafloor sediments at this time [data S1; (*4*, *18*, *32*)].

Middle Cambrian to upper Silurian shallow marine successions, although recording gradual increases in bioturbation depths and intensities, are similarly characterized by a combination of high intensities of horizontal burrowing and low intensities of vertical sediment mixing. Trace fossils of centimeter-scale diameters are common, occur in dense multigenerational assemblages, and record sophisticated strategies of infaunalization (*35*, *37*, *38*). However, bed-penetrative burrowing is relatively uncommon and does not exceed millimeter- to centimeter-scale depths; burrow assemblages are commonly shallow tier and exceptionally preserved (*35*). Moreover, although thicker, on average, than in lower Cambrian successions, tempestites remain remarkably thin; for instance, mean sandstone bed thickness in heterolithic siliciclastic successions has been reported to not exceed 3.5 cm [data S1; (*35*, *36*, *39*)]. In both siliciclastic and carbonate successions that record shallow subtidal environments, sedimentary fabrics are only moderately disrupted; although rare intervals are characterized by ii values as high as 5, mean ii in many heterolithic siliciclastic and carbonate successions does not exceed 3.5 [data S1; (*4*, *11*)]. The only early Paleozoic shallow subtidal marine environment in which sediment mixing appears to have undergone a major expansion in intensity and depth was carbonate inner shelf systems—for instance, mean ii values substantially increase between Middle and Upper Ordovician strata in the Great Basin of the western United States (from ii 3.1 to ii 4.6) [data S1; (*40*)]. However, through most of the early Paleozoic—as constrained by data from lower Cambrian to upper Silurian heterolithic siliciclastic systems and lower Cambrian to Middle Ordovician carbonate systems—sediment mixing remained relatively limited in shallow marine settings. On the basis of these data, the mixed layer has been suggested to have experienced, on average, only modest increases in depth across this interval (for instance, from approximately 0.2 to 1.5 cm in heterolithic siliciclastic settings) (*4*, *11*, *35*).

Middle to late Paleozoic sediment mixing

Detailed studies of sediment-mixing intensity in middle to upper Paleozoic successions are relatively rare. Trace fossil assemblages and sedimentology of the Lower Devonian (Pragian to Emsian) Teferguenite Formation in the Ougarta Range of Algeria record high ichnodiversity but variable intensities of sedimentary fabric disruption (*41*). Correlative Lochkovian to Emsian strata of the Reggane Basin of Algeria are dominated by unbioturbated mudstone hosting variably bioturbated sandstone and carbonate interbeds inferred to record shoreface settings (*42*). These interbeds range from poorly bioturbated [Bioturbation Index (BI) 2] and low-ichnodiversity strata dominated by *Planolites* or *Skolithos* to moderately to intensely bioturbated (BI 4 to 5) *Skolithos*-, *Thalassinoides*-, and *Chondrites*-dominated ichnofabrics (*42*). However, these intensively bioturbated intervals are exceedingly rare; 86% of strata in this 430-m succession

are unbioturbated; 7% are characterized by BI 2, 7% by BI 4, and <1% by BI 5 [data S1; (*42*)]. These data suggest that although infaunalization was well advanced in certain settings and infauna were capable of high levels of sedimentary fabric disruption, intensive and deep sediment mixing was not yet widespread during the Early Devonian. A previous study of Upper Devonian through Carboniferous platform, shelf, backbulge, and foreland basin and upper slope carbonate deposits in the Great Basin and Rocky Mountain regions of the western United States (*43*) has also suggested that bioturbation in the Frasnian was low, with a mean ii of 2.0 (data S1). Although some intervals of these Frasnian successions are more intensely bioturbated (ii 3 to 5), they account for less than 30% of measured strata and, with limited exception, beds that are vertically mixed rarely exceed 10 cm in thickness. Discrete trace fossils are uncommon in the Frasnian of these western US successions but include *Thalassinoides*, *Chondrites*, and *Planolites*. Bioturbation appears to have further decreased in the Famennian (data S1), with a mean ii of just 1.6. In these deposits, 76% of strata have an ii of 1 and only 17% have an ii of 3 or above. The contrast between Frasnian and Famennian strata in these regions is particularly notable given the broad similarity of facies recorded in each interval. Discrete trace fossils are rare in the Famennian part of this succession; only a few *Chondrites* are visible and evidence of vertical mixing in these beds is largely absent. Recorded bioturbation intensity increases in the Mississippian intervals of these successions but remains fairly low with a mean ii of only 2.2 (data S1). However, nearly 40% of Carboniferous strata in these successions have an ii of 3 to 5 and trace fossil assemblages are more variable and diverse, suggestive of major expansions in vertical mixing accompanying local increases in burrow network depth. In the Carboniferous part of this succession, skeletal debris is pervasive, which may have impeded more intense bioturbation or may, alternatively, simply hamper recognition of bioturbated fabrics and discrete trace fossils (*43*).

Although limited in extent, those data available from preextinction Permian strata recording shallow marine settings contain densely packed ichnoassemblages populated by diverse ichnofauna inferred to record a range of feeding strategies (*44*, *45*). Permian epicontinental carbonate deposits (e.g., the Kaibab Formation of the western United States) are characterized by well-mixed fabrics overprinted by silicified *Thalassinoides* burrow networks representing secondary transition layer colonization of previously reworked and buried mixed layer sediments (*46*). Data from upper Permian (Changhsingian) strata suggest that shallow subtidal marine sediments in at least some regions were intensely mixed and even completely homogenized; for instance, ichnofabric analysis of uppermost Permian strata of the Austrian Alps has indicated that ichnofabric indices of 5 to 6 are prevalent through this interval [data S1; (*45*, *47*)].

Triassic–Jurassic sediment mixing

After an earliest Triassic (Griesbachian) substantial decrease in bioturbation following the end-Permian extinction (see below), the intensity and depth of sediment mixing, along with burrowing depth, gradually increased. Despite ephemeral increases in mixing intensities [e.g., up to ii 5 in Dienerian intervals of the Werfen Formation of Italy; data S1; (*45*, *47*)], bioturbation did not recover to preextinction levels until the latest Early (Spathian) to Middle Triassic, with continued recovery into the Late Triassic (*45*). This increase has been interpreted to signify a full (albeit protracted) recovery of benthic ecosystems from the end-Permian mass extinction (*48*). This recovery eventually resulted in a return to Permian levels of sediment mixing, as indicated by increasing mean thicknesses of preserved event beds (*49*) and moderate to high ichnofabric indices (*45*). Following local decreases across the Triassic-Jurassic boundary, sediment-mixing intensities appear to have rebounded during the Hettangian–Sinemurian Ages of the Early Jurassic [data S1; (*45*)]. Although previous studies have suggested that increased infaunal ecospace utilization associated with the Mesozoic Marine Revolution (MMR) initiated in the Triassic and Jurassic (*50*, *51*), records of coeval sediment-mixing depths and intensities are sparse. The available data support deepening of the mixed layer across this interval, as indicated by the disappearance of very thin event beds from the shallow marine record, which were preserved in shelf settings until the Jurassic but not subsequently (*49*). Further evidence for a Jurassic deepening of the mixed layer includes an increase in the relative abundance of completely homogenized, mottled, or massive strata (*36*) and body fossil records of the middle Mesozoic diversification of important bulldozing and sediment-mixing groups (*50*, *52*).

Cretaceous–Cenozoic sediment mixing

Both body and trace fossil records suggest that the radiations in active, deep-burrowing infauna, and likely associated increases in sediment reworking rates and depths, that commenced in the Jurassic continued into the Cretaceous and Cenozoic (*36*, *52*–*55*). These records indicate that, throughout the Cretaceous, the majority of offshore and shelf sediments were completely homogenized by biogenic mixing, suggesting that shallow subtidal mixed layers were relatively deep during this interval [data S1; (*56*)] and that, even in comparatively high-energy shallow marine settings, rates of bioturbation commonly outpaced rates of sediment accumulation.

Stratigraphic characterization of Mesozoic and Cenozoic platform facies indicates that much of this record is characterized by fine-grained sandstones, carbonates, and sandy shales with mottled, homogenized, and massive textures resulting from bioturbation (*36*). Mesozoic–Cenozoic platform deposits are characterized by well-bioturbated fabrics similar to those of Paleozoic and younger nearshore (littoral) deposits (*36*). Primary sedimentary structures are relatively rare in Cretaceous and Cenozoic shallow marine deposits; where these are preserved, they have largely been linked to either unusually large storm events (and deposition of thick, decimeter-scale tempestites) (*36*, *56*) or protracted intervals of water-column anoxia, as appear to have occurred repeatedly in the Western Interior Seaway of North America (*56*). Cretaceous chalks deposited in epicontinental settings are commonly completely bioturbated (*57*, *58*). Shallow burrows and surficial structures have been entirely overprinted, and surviving ichnoassemblages are dominated by transition layer structures formed by deep-burrowing infauna (*58*). In shelf settings, recognition of these transition-layer ichnofossils is commonly enhanced by secondary mineralization, particularly silicification (*58*) or early diagenetic concretion formation (*36*). Conversely, bioclastic deposits and tempestites are relatively rare in deposits of this age and are commonly linked to exceptional preservational circumstances (*36*). Changes in brachiopod morphology, abundance, and diversity indicate that late Mesozoic (particularly Late Jurassic to Cretaceous) and Cenozoic increases in sediment-mixing depths and intensities initially drove a shift in brachiopod habitats from fine-grained siliciclastic sediments to carbonate-dominated settings characterized by firmer sediments and eventually led to widespread exclusion (*59*). Compilations of ichnogenera classically associated with more intensive sediment-reworking modes likewise suggest that a major increase in sediment-mixing intensity, comparable to

modern levels of sediment mixing, initiated in the Cretaceous and continued into the Cenozoic (*60*).

Cenozoic hyperthermal perturbations, such as the Paleocene–Eocene Thermal Maximum (PETM), appear to have variably affected bioturbation intensities (data S1). At Mead Stream and Dee Stream, New Zealand, for instance, the onset of the negative carbon isotope excursion that defines the base of the PETM coincides with a cessation of bioturbation (as measured by trace fossil abundance in sedimentary ichnofabrics) in the upper continental slope deposits of the Amuri Limestone, potentially reflecting a protracted initial interval of hypoxia (*61*). However, at Bass River, off the New Jersey Coastal Plain, bioturbation appears to have continued through the PETM (*62*). Both magnitude of warming and synergistic feedbacks between warming and other environmental factors, such as oxygen bioavailability and nutrient loading, may therefore have played a key role in shaping sediment-mixing responses across this hyperthermal.

The shallow marine transition layer and the development of deep-tier burrowing

The abundance of reported burrow depth measurements from strata that collectively span much of the Phanerozoic, including for trace fossil taxa typically associated with the deepest tiers of burrowing, allows for quantitative analysis of patterns in Phanerozoic transition layer development to an extent not currently possible for coeval mixed layer development. In particular, these data facilitate investigation of when and in what depositional environments deep burrowing became a common ecological strategy, allowing us to reassess patterns previously proposed by studies focused on the Phanerozoic evolution of infaunal tiering (*12*–*14*). The dataset compiled here contains 365 measurements of the maximum reported vertical extent of the trace fossils *Arenicolites*, *Diplocraterion*, *Ophiomorpha*, *Skolithos*, *Thalassinoides*, and *Zoophycos* from lithified sedimentary units (Fig. 2). We include an additional 25 measurements of the depth of these traces in unlithified sediments. Each maximum burrow depth provides a snapshot of the estimated depth of the transition layer in a particular sedimentary unit and at a particular time. These data, and references for the studies from which they were collated, are included in data S2.

There is substantial variability in maximum burrow depths across the Phanerozoic (Fig. 3). Linear, exponential, and logarithmic models do not provide strong fits for the unbinned dataset.

Sampling is not even throughout the Phanerozoic; in particular, only sparse data are currently available for the middle Paleozoic and for the Middle to Upper Triassic. Silurian data are so sparse that we have excluded this system from some analyses. These time intervals remain distinctly undersampled even after normalizing the number of observations in our burrow depth dataset to available outcrop area or time bin duration (fig. S1). Conversely, the Lower Triassic recovery interval following the Permian-Triassic mass extinction is extremely well sampled. To address both this particular sampling bias and assess the potential influence of mass extinction events on burrow depths over the Phanerozoic, all analyses were also performed without measurements from strata correlative with the "Big Five" extinctions and subsequent recovery intervals, but removal of these extinction-associated burrow depth data had no substantive effect on the resulting trends.

Transition layer depths reconstructed from these burrow depth data are relatively consistent throughout the Paleozoic (Fig. 4). The comparative paucity of Upper Devonian data may contribute to the slight decline in transition layer depth we observe in the Middle Devonian part of our dataset. The transition layer appears to have experienced notable deepening between the Middle Triassic and

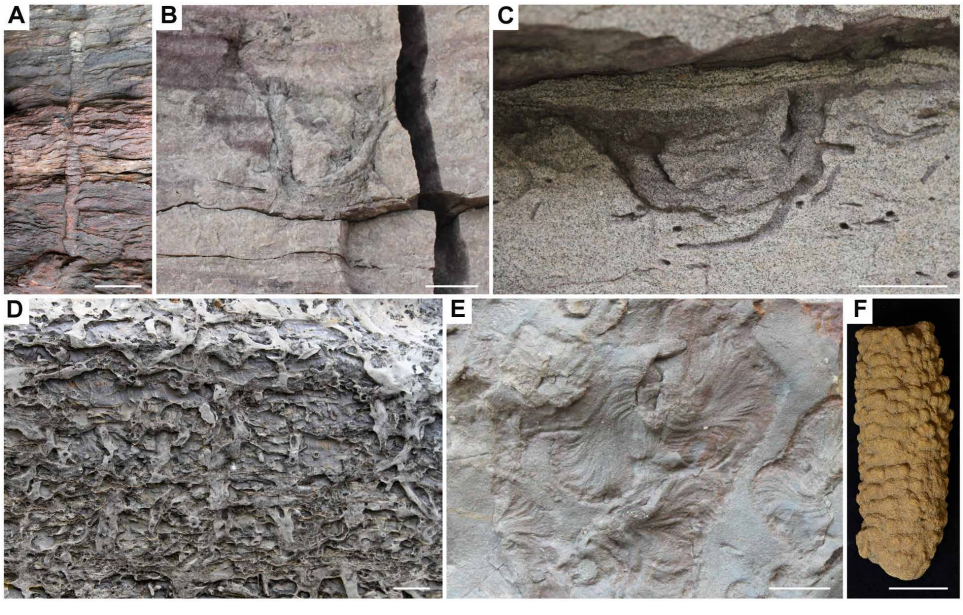

Fig. 2. Examples of the six deep-penetrating ichnotaxa used to generate our estimates of transition layer depth through the Phanerozoic. (**A**) *Skolithos*, Ordovician Powers Steps Formation (Newfoundland, Canada). (**B**) *Arenicolites*, Cambrian Hawke Bay Formation (Newfoundland, Canada). (**C**) *Diplocraterion*, Cambrian Lodore Formation (Utah, USA). (**D**) *Thalassinoides*, Ordovician Boat Harbor Formation (Newfoundland, Canada). (**E**) *Zoophycos*, Silurian Clinch Formation (Virginia, USA). (**F**) *Ophiomorpha*, Cretaceous Fox Hills Formation (South Dakota, USA). (D) Modified from (*11*). (F) Specimen YPM IP 150791, photo courtesy of the Yale Peabody Museum, Division of Invertebrate Paleontology, Yale University; peabody.yale.edu. (A to D and F) Cross section; (E) bedding plane. Scale bars, 2 cm.

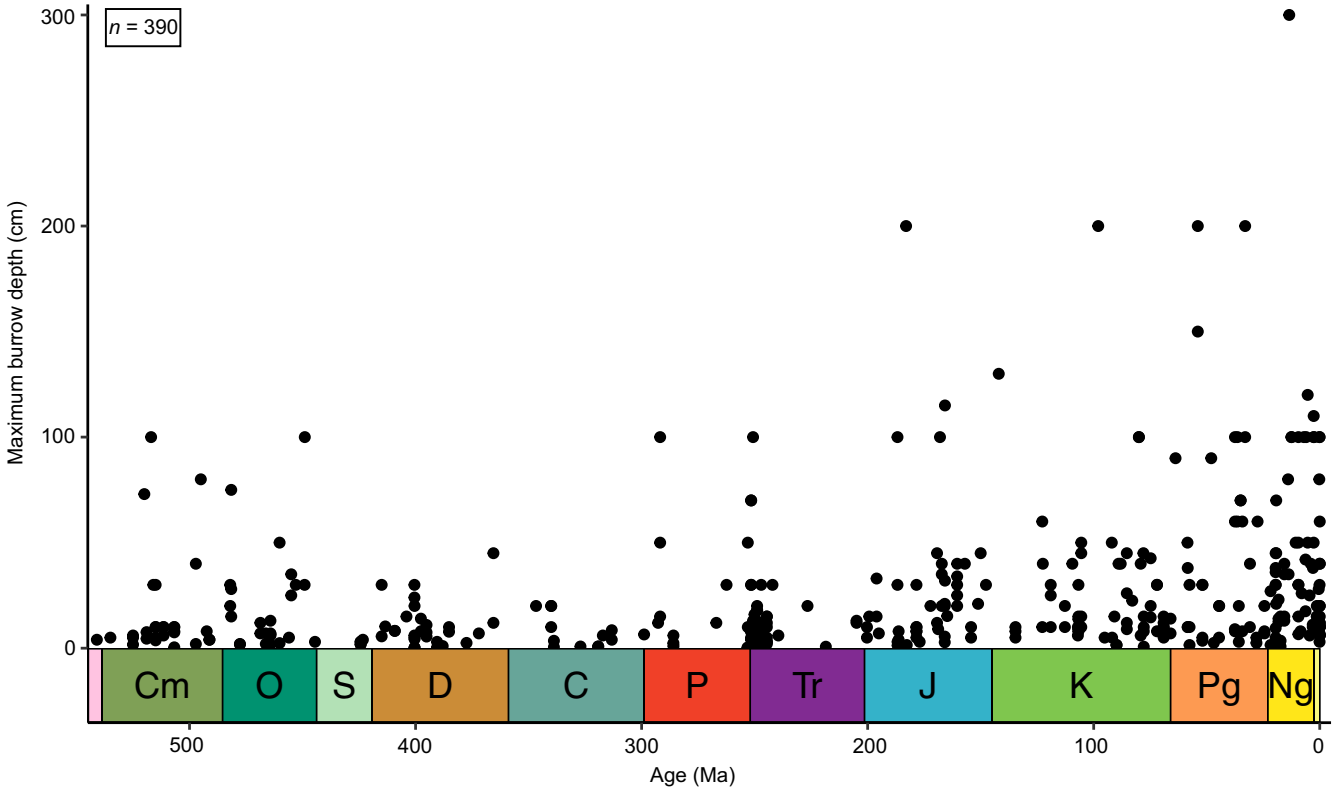

Fig. 3. Maximum burrow depths included in this study. Each data point is the maximum vertical extent reported by individual publications for one of the six ichnotaxa included in this study. Geological timescale visualized using the R package deeptime (v1.1.1) (*114*).

Middle Jurassic (Fig. 4). Changepoint analyses detect a prominent stepwise increase in transition layer depth in the Early to Middle Jurassic (Fig. 5). A second deepening of the transition layer appears to have taken place during the Paleocene and Eocene (Fig. 4), coincident with a second stepwise increase shown in the changepoint model at the Paleocene-Eocene boundary (Fig. 5). Less evident in a LOESS (locally estimated scatterplot smoothing) model, but still apparent as a substantive changepoint, is a third stepwise increase in transition layer depth recorded in middle Miocene strata (Fig. 5). We describe ichnotaxon-specific patterns in burrow depth and general patterns in Paleozoic, Mesozoic, and Cenozoic transition layer evolution in greater detail below.

Ichnotaxonomic patterns in transition layer evolution

Different ichnotaxa display different depth patterns over the Phanerozoic and some changes in maximum transition layer depth may be attributable to a deepening of burrows of a particular ichnotaxon. More than half of the burrows with uncorrected depths >12 cm in our Paleozoic transition layer dataset are *Skolithos* (60.7%; note these raw burrow depth values do not consider compaction; we hereafter refer to these as "uncorrected"; see below for further discussion of compaction). In Mesozoic and Cenozoic strata, only 16.4 and 20.0%, respectively, of burrows >12 cm uncorrected depth are *Skolithos*. Across the Phanerozoic, sedimentary units contain both very deep and shallow *Skolithos*; the range of maximum reported *Skolithos* depths appears to be relatively invariant through time. This is further supported by the lack of substantive changepoints in *Skolithos* burrow depths and the consistency of the *Skolithos* average model (Fig. 6). *Thalassinoides* also exhibits relatively consistent models of maximum burrow depth over the Phanerozoic, although this is the trace fossil characterized by the sparsest depth data (Fig. 6).

The Mesozoic increase in transition layer depth is associated with notable increases in the depth of the U-shaped burrows *Arenicolites* and *Diplocraterion*, as well as the appearance and expansion of *Ophiomorpha* (Fig. 6). The presence of *Ophiomorpha* in Mesozoic and Cenozoic strata is associated with some of the deepest transition layers that emerged from our dataset. No individual ichnotaxon emerges as the dominant driver of transition layer depth in our Mesozoic dataset, but *Ophiomorpha* represents 48.0% of burrows recording transition layers >12 cm in the Cenozoic. Substantial increases in maximum *Ophiomorpha* depth are associated with positive changepoints (i.e., detected increases) in transition layer depth both across the Paleocene–Eocene transition and during the Miocene (Fig. 6). *Zoophycos* is characterized by a prominent changepoint (and increase in burrow depth) in the Cretaceous.

Paleozoic transition layer depths

In shallow subtidal marine environments, a deep transition layer appears to have been established relatively rapidly following the latest Ediacaran and early Cambrian emergence of vertical burrowing (Fig. 4). In our dataset, very deep burrows first appear in Cambrian Stage 3, indicating that deep-tier burrowing, like other forms of infaunalization (*28*, *31*), was well advanced across a range of shallow marine settings by the early Cambrian. Transition layers dominated by deep-tier burrows [>12 cm depth; compare to (*14*)] are more abundant in the lower Paleozoic part of our dataset relative to some subsequent Paleozoic intervals (e.g., 41.0% of Cambrian and Ordovician transition layers reach deep infaunal tiering levels).

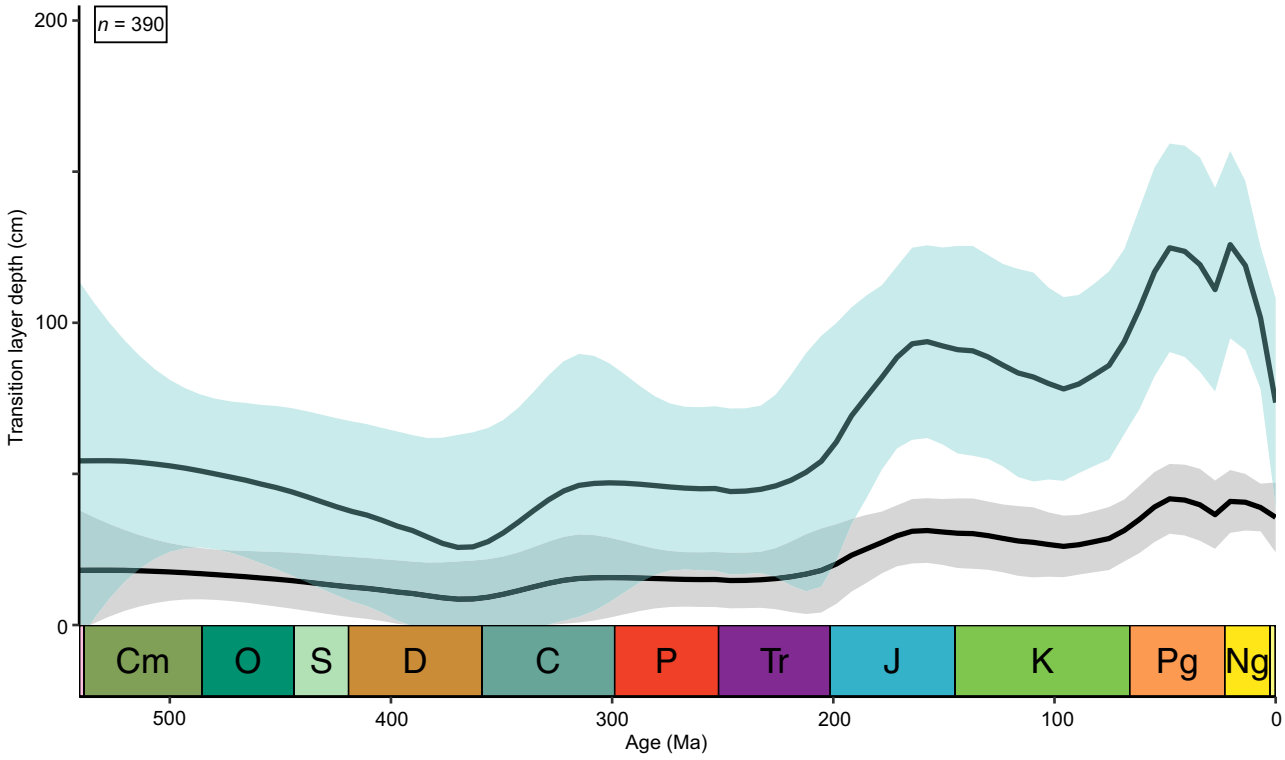

Fig. 4. Transition layer depth over the Phanerozoic. Gray lower curve reflects data with a lower-bound decompaction factor of 1.0 applied; green upper curve reflects data with an upper-bound decompaction factor of 3.0 applied. Curves produced by LOESS smoothing model with $\alpha = 0.3$. Shaded areas are 95% confidence intervals. Geological timescale visualized using the R package deeptime (v1.1.1) (*114*).

However, these are largely restricted to specific ichnofabrics, facies, and paleoenvironments—including (i) *Skolithos*- and, in some instances, *Arenicolites*- or *Monocraterion*-dominated densely packed assemblages or "piperock" in sandstones recording proximal subtidal and nearshore settings (*63*–*65*); (ii) Ordovician *Daedalus*-dominated assemblages in nearshore and shoreface sandstones (*66*); and (iii) Ordovician *Thalassinoides* networks in carbonate inner shelf environments (*40*). In addition, lower Paleozoic maximum uncorrected burrow depths have a median value of 7.6 cm (25th percentile = 4.5 cm, 75th percentile = 28.0 cm). These results are largely consistent with findings that, although present in certain shallow marine settings and geologic successions, large vertical burrows are relatively uncommon in Cambrian strata; ichnofabrics in these successions are more commonly dominated by meiofauna-scale and small macrofaunal burrows (*31*, *33*, *35*).

Transition layers dominated by deep-tier burrows remain relatively uncommon after the Ordovician (only 26.1% of Silurian–Permian transition layers include a "deep" infaunal tier). Median values of maximum uncorrected burrow depths are 7.0 cm (25th percentile = 3.0 cm, 75th percentile = 11.0 cm) in middle Paleozoic strata and 8.5 cm (25th percentile = 2.4 cm, 75th percentile = 20.0 cm) in upper Paleozoic strata. Our analyses do not indicate a substantial increase in the depth of the transition layer in the middle to late Paleozoic (Fig. 5), in contrast to previously proposed patterns in infaunal tiering (*13*, *14*). These results suggest that although some groups of infauna (e.g., some groups of anomalodesmatan and pholadomyoid bivalves and some crustaceans) were capable of occupying deep tiers by the middle and especially the late Paleozoic (*14*)—as highlighted by previous studies tracking changes in tier occupation (*14*) and as evidenced by the increase in the 75th percentile of burrow depths in our dataset by the upper Paleozoic—this was not yet a common life mode. This lag in abundant inhabitation of this deepest tier may reflect limited ecological incentives (e.g., lower predation pressure) to exploit deeper sediment tiers—a potential driver that we explore in greater detail below, in conjunction with discussion of Mesozoic transition layer evolution. However, this interval also contains the fewest observations in our dataset [when normalized to period duration and outcrop area (fig. S1)], so further exploration of the trace fossil record of the middle to upper Paleozoic, including further assessment of ichnotaxa that have been attributed specifically to deep-burrowing bivalves, may help expand our understanding of transition layer depths through this interval.

Mesozoic transition layer depths

Our dataset shows a sharp increase in reconstructed transition layer depths beginning at the end of the Middle Triassic and continuing through the Jurassic (Figs. 4 and 5), which we propose may have been concurrent with the onset of increased infaunal ecospace utilization associated with the MMR. The proportion of transition layers that can be classified as deep tier [compare to (*14*)] rises slightly in the Triassic (from 34.1% in the Paleozoic to 37.1% in the Triassic) before jumping to 57.1% in the Jurassic and 65.9% in the Cretaceous. Synchronously, the median value of maximum uncorrected burrow depth increases from 8.0 cm (25th percentile = 3.0 cm, 75th percentile = 15.2 cm) in Triassic strata, a range consistent with Paleozoic burrow depths, to 17.6 cm (25th percentile = 8.0 cm, 75th percentile = 32.8 cm) in Jurassic strata and 15.0 cm (25th

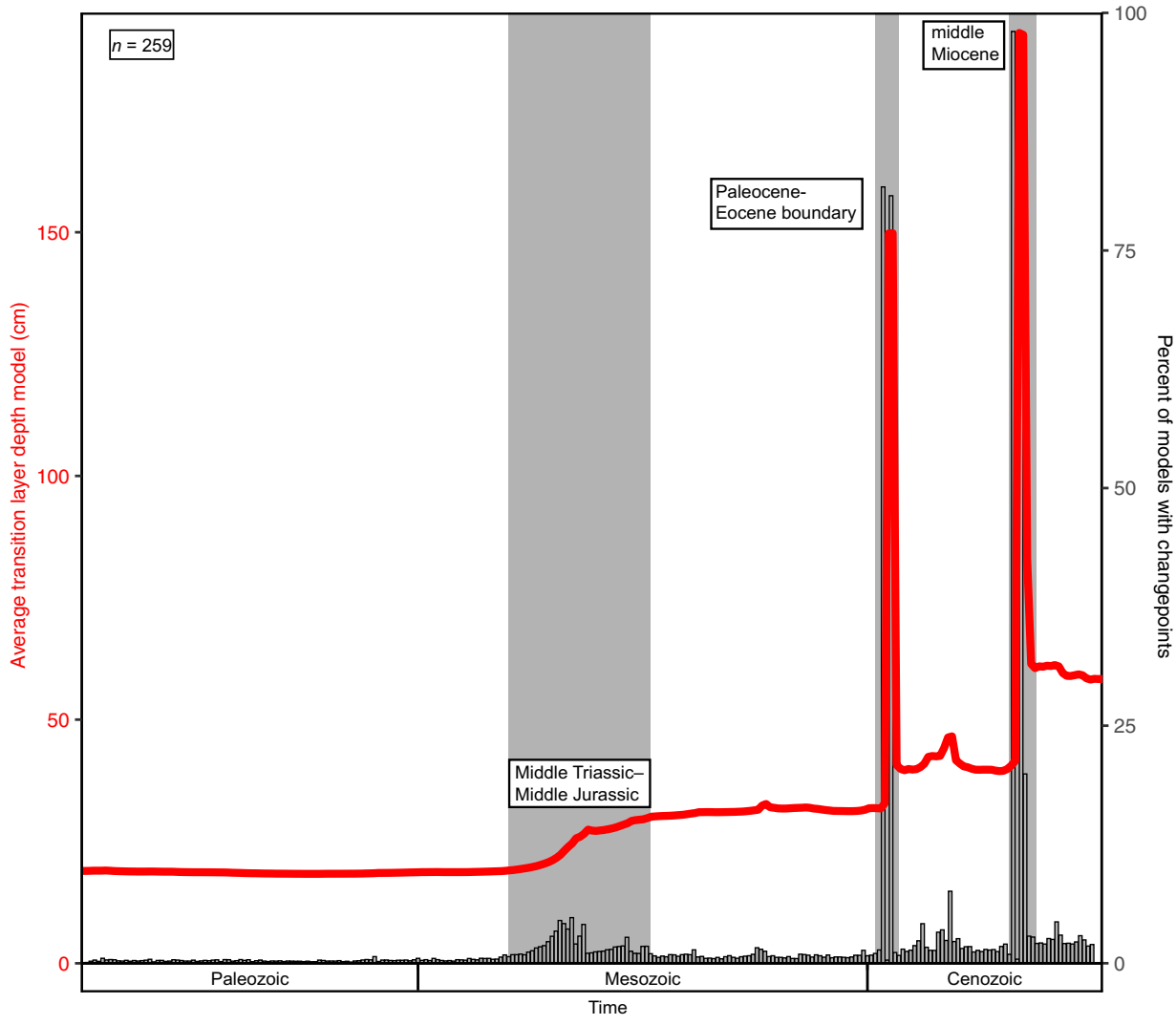

Fig. 5. Results of changepoint analysis for maximum transition layer depths over the Phanerozoic. Transition layer depths are normalized to the reported stratigraphic unit and are arranged in chronological order following a null model of uniform distribution (see Materials and Methods for further description of changepoint analyses). No decompaction factors have been applied and burrows from unconsolidated sediments are not included. Bar heights indicate the number of changepoint model runs that identify a changepoint at the point in time indicated by the burrow's position in the chronological uniform model; red curve is the average model of transition layer depth computed across the Phanerozoic.

percentile = 9.8 cm, 75th percentile = 40.0 cm) in Cretaceous successions. Although evidence for the onset of the MMR has been historically drawn from Jurassic increases in shell ornamentation and thickness in epibenthic mollusks (*55*), other work has highlighted a potential Late Triassic initiation of the MMR, reflected in part by shell morphological changes facilitating increased mobility and infaunalization in other mollusk groups (*51*). These morphological changes have been proposed to record an escalation of avoidance strategies in response to the Triassic evolution of shell-breaking and -crushing predators (homaridean lobsters and shell-crushing fish) that feed at the sediment-water interface and at very shallow sediment depths (*67*). Our trace fossil data corroborate Triassic body fossil observations by providing first-order evidence for late Middle Triassic increases in burrowing depth.

In addition, our dataset suggests that a wider range of animals than mollusks may have started to occupy deeper tiers of the seafloor as far back as the Late Triassic and, more broadly, highlights disparate timing of deep-tier colonization among different taxonomic and ecological groups of infauna, including soft-bodied taxa unlikely to be represented in Mesozoic body fossil records. For instance, the maximum uncorrected burrow depths of *Arenicolites* and *Diplocraterion* increase in Upper Triassic strata (Fig. 6). In contrast, we observe that *Thalassinoides* burrow depths increase in Upper Jurassic strata. These initial increases are followed by more substantial increases in burrow depth in Jurassic (*Arenicolites and Diplocraterion*) and Paleogene (*Thalassinoides*) strata (Fig. 6). Diagnosing the taxonomic affinities of infauna from the trace fossil record is challenging, as a single trace may have multiple taxonomically distinct progenitors and a single organism may also create multiple traces while engaging in disparate behaviors (see the Supplementary Materials for further discussion). Nonetheless, some broad-scale taxonomic relationships can be discerned. Modern examples of *Ophiomorpha* are

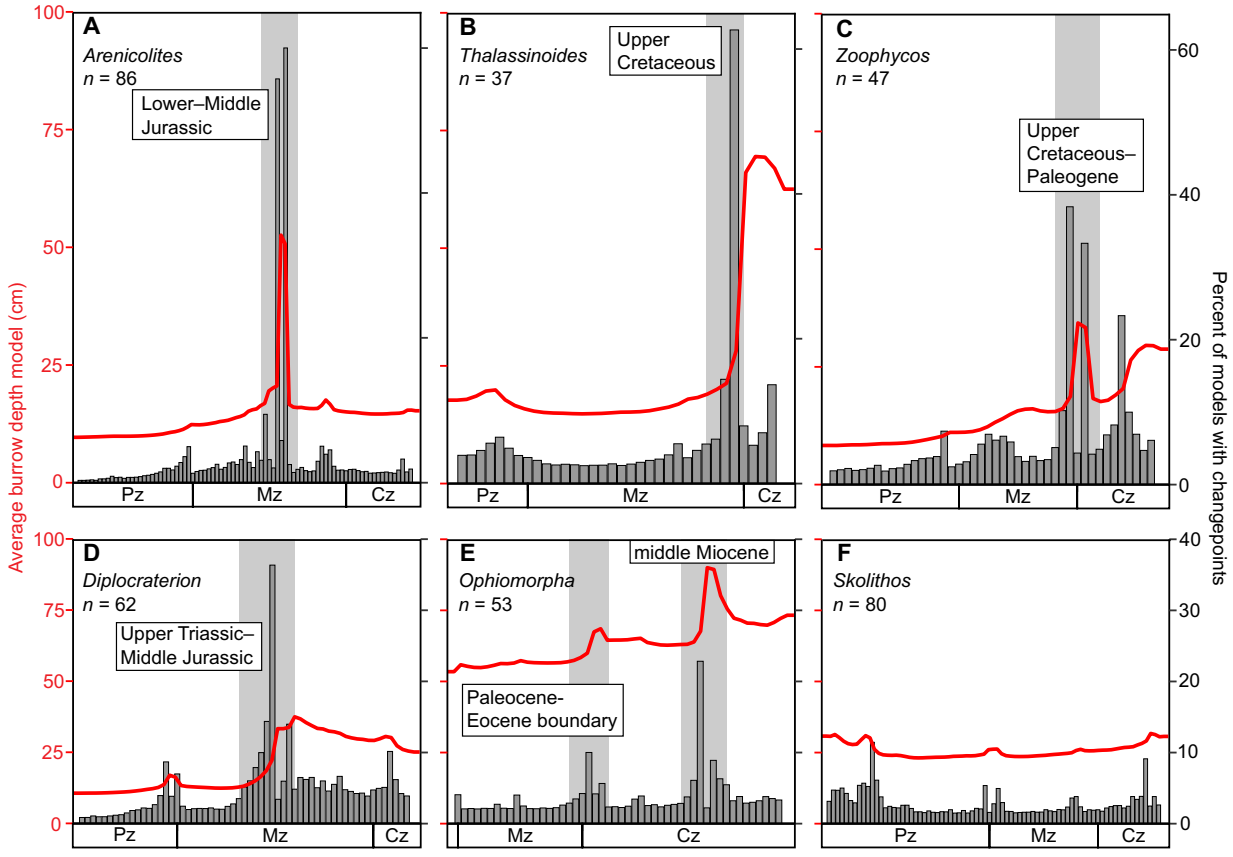

Fig. 6. Changepoint analyses of Phanerozoic trends in maximum burrow depth for each of the six ichnotaxa included in our study. (**A**) *Arenicolites*. (**B**) *Thalassinoides*. (**C**) *Zoophycos*. (**D**) *Diplocraterion*. (**E**) *Ophiomorpha*. (**F**) *Skolithos*. Burrow depths are arranged in chronological order following a null model of uniform distribution (see Materials and Methods for further description of changepoint analyses). No decompaction factors have been applied and burrows from unconsolidated sediments are not included. Bar heights indicate the number of changepoint model runs that identify a changepoint at the point in time indicated by the burrow's position in the chronological uniform model; red curve is the average model of burrow depth computed across the Phanerozoic. Note the differences in *x*-axis scale between the different panels and the difference in *y*-axis scale between the top and bottom rows of panels.

commonly attributed to the burrowing activities of deposit-feeding decapod crustaceans such as mud and ghost shrimp, which first appeared during the Early Jurassic (*68*, *69*). *Ophiomorpha* burrows, which first appear in Permian strata, become common in our dataset in Jurassic strata and rapidly reach large maximum depths (Fig. 6). Increases in *Ophiomorpha* abundance may therefore, as discussed below, be associated with mid-Mesozoic shifts in seafloor nutrient supply and distribution. Some groups of infaunal worms also experienced increases in diversity during the MMR (*70*); in particular, the Arenicolidae, the family that contains the large and deep-burrowing lugworms, is known from the Triassic onward. Younger examples of large *Arenicolites* have commonly been attributed to the burrowing activities of lugworms, and we observe an increase in the relative abundance of very large *Arenicolites* starting in the Lower Jurassic (and given the scarcity of published Upper Triassic burrow depth data, slightly earlier increases may also be feasible). As discussed above, assessment of additional burrow morphotypes associated with other members of the Modern Evolutionary Fauna [compare to (*54*)] may, in the future, reveal additional insights.

Enhanced predation pressure upon (and potentially also from) newly infaunalizing groups (discussed above) and associated changes in resource partitioning may have incentivized tracemakers of the ichnotaxa in our dataset to explore greater depths of seafloor sediments. The Mesozoic (particularly the Jurassic–Cretaceous) is also associated with a major shift in phytoplankton community composition, which has been proposed to have increased rates and efficiencies of upward transfer of energy and facilitated the emergence of larger size classes (*71*). In addition, carbonate I/Ca records have been inferred to reflect Mesozoic (and potentially Jurassic) increases in seawater oxygen levels (*72*). As burrowing is a metabolically demanding activity, increased food availability and more efficient growth rates, as well as increased oxygen bioavailability, resulting in larger body sizes and higher metabolic indices, would have eased some of the physiological pressures on both deep-tier burrowing and deep sediment mixing. These two factors could therefore provide an additional explanation for Triassic–Jurassic increases in transition layer depths, as well as Jurassic and Cretaceous increases in mixed layer depths.

Cenozoic transition layer depths

Previous analyses of both body and trace fossil records suggest that radiations in actively and deeply burrowing infauna and associated increases in feeding depths that commenced in the Jurassic continued into the Cretaceous and Cenozoic (*36*, *52*–*55*). Our dataset reflects this in that the shift to deeper maximum transition layer

depths first observed in Mesozoic strata persists and even increases in Cenozoic strata (Figs. 4 and 5). For instance, 82.0% of transition layers reached deep infaunal tiering status in the Cenozoic, and maximum burrow depths that would have been exceptional in previous intervals become relatively common. The median value of maximum burrow depth reaches its highest point in Cenozoic strata, and burrows with uncorrected depths of more than 50 cm in lithified strata are common by this interval (median = 30.0 cm, 25th percentile = 10.0 cm, 75th percentile = 60.0 cm).

The higher resolution of the Cenozoic record of bioturbation, facilitated by the greater available area of sedimentary outcrops and seafloor sediments, permits the recognition of smaller-scale shifts in transition layer depth during this interval, including the identification of shifts not detected by earlier studies that interrogated patterns in infaunal tiering depths (*12*, *14*). Intriguingly, the two Cenozoic-aged stepwise shifts that emerged from our changepoint model are both associated with major warming events; the first occurs at roughly the same time as the PETM, and the second coincides with the mid-Miocene Climate Optimum (MCO).

We observe a substantial deepening of the transition layer in strata recording shallow subtidal environments across the PETM (Fig. 5). Deeper burrows may have been an adaptation to escape warmer ocean bottom-water temperatures during this hyperthermal, particularly for shallow-water communities adapted to bottom-water temperature oscillation on daily and seasonal timescales. These greater burrow depths may have persisted and expanded among survivors following the end of the PETM; modern experimental work has suggested that some infaunal taxa, including polychaetes and cardiid bivalves, may burrow to substantially greater depths at higher temperatures (*73*, *74*), as deeper burrows may, in shallow water settings, buffer higher daytime temperatures (see the Supplementary Materials for additional discussion). This PETM trend in burrow deepening is most evident among *Ophiomorpha* and, to some extent, *Thalassinoides* burrows (there are no *Thalassinoides* in our dataset from Paleocene strata—but Eocene and Oligocene *Thalassinoides* penetrated substantially deeper than Mesozoic *Thalassinoides*; Fig. 6). Both *Ophiomorpha* and *Thalassinoides* are classically associated with decapod crustaceans, which radiated in the Eocene (*75*, *76*). This radiation is considered to have resulted in increased abundance and perhaps increased depth of decapod-produced trace fossils (*50*, *77*).

An additional increase in *Ophiomorpha* depths is observed in middle Miocene strata; this trace alone is responsible for the overall increase in maximum transition layer depth we reconstruct for this time (Figs. 4 and 6). Although the middle Miocene was a warm period, the MCO was not a hyperthermal. Deeper *Ophiomorpha* may therefore reflect the specific thermal or ecological preferences of its decapod tracemakers, rather than the operation of warming-driven selective pressures at an ecosystem scale. The Miocene was also characterized by increases in decapod diversity (*76*) and Neogene strata contain a high abundance of decapod trace fossils (*50*, *77*); middle Miocene increases in transition layer depth and the subsequent shift to higher baseline values may simply reflect this evolutionary radiation rather than responses to shifts in climate state. The timing and extent of these Cenozoic increases in transition layer depth merit further investigation, including exploration of whether there are increases in the depth of trace fossils beyond the six ichnotaxa we explore in this study.

The lack of apparent oscillations in transition layer depth before the Cenozoic cannot be interpreted to reflect a static Paleozoic transition layer or Mesozoic invariance in transition layer depth beyond the major MMR-associated increase discussed above. It is very likely that transition layer depths also responded to climate perturbations and state shifts, as well as to radiation and extinction events among other infaunal groups, throughout the Paleozoic and Mesozoic. However, the coarser resolution of the Mesozoic and especially the Paleozoic sedimentary record hampers recognition of more transient or smaller-scale shifts in transition layer depth. Further investigation of understudied intervals of the Phanerozoic is imperative for recognition of additional potential shifts in transition layer depth.

Bioturbation across mass extinctions

Long-term trends toward deeper burrowing and more intensive sediment mixing have been pronounced but not continuous. In particular, mass extinction events and their aftermaths appear to have been frequently associated with environmental stressors that markedly reduced sediment mixing and limited burrowing depths—particularly in midshelf habitats—in some cases for several million years, though recovery from these episodes was not universally associated with state shifts in the depth of either the mixed or transition layers.

The late Permian mass extinction and subsequent Early Triassic recovery interval provide the most comprehensive record of changes in sediment mixing in the aftermath of a global biotic crisis. As noted above, in many lowermost Induan deposits recording midshelf settings, the trace fossil record is dominated by diminutive (1 to 5 mm diameter) horizontal burrows formed by infauna that reworked only the sediment surface or by vertical burrows that penetrated <1 cm below the sediment-water interface (*45*, *47*, *78*). Burrowing depth was highly limited for >1 million years (Myr) following the extinction, with incipient but ephemeral recoveries during less environmentally stressful intervals. Olenekian strata record increases in burrow depths (e.g., to 5 to 10 cm), but it was not until the Middle Triassic, some 5 Myr after the extinction, that vertical burrows routinely reached depths of greater than 10 cm (*79*) and, as described above, prominent increases in transition layer depth appear in the sedimentary record. Dramatic latest Permian declines in bioturbation and the protracted pace of recovery in Triassic deep-burrow construction and sediment-mixing depths and intensities, relative to other hyperthermal episodes such as the PETM, may reflect particularly severe thermal stress (which may have been especially pronounced for infauna acclimated to late Paleozoic icehouse conditions). Alternatively, variation in the severity of impacts on bioturbators recorded across different Permian–Triassic sections (see below) and across other hyperthermals may reflect disparities in the extent to which warming was compounded by synergistic feedbacks with other environmental stressors, such as deoxygenation (*45*) and nutrient loading (see the Supplementary Materials for additional discussion).

The intensity of sediment mixing during the Early Triassic postextinction recovery interval appears to have varied considerably across environments (*80*). Patterns of recovery, however, appear to have largely recapitulated broader-scale Paleozoic trends in the evolution of bioturbation (*81*), with a protracted increase from no to minimal levels of bioturbation in the Induan to moderate to intense levels of sediment mixing, typical of the preextinction upper Permian record, in the Middle Triassic (*79*). Exceptional preservation of bioglyphs (tracemaker "fingerprints" such as scratch marks) associated with shallow-tier and surficial structures such as arthropod traces and swim tracks (trackways formed by buoyant to semibuoyant tetrapods moving across a submerged substrate), in conjunction with

low ichnofabric indices, indicate that cohesive and poorly bioturbated firmgrounds were prevalent in shallow marine and deltaic settings during this recovery interval (*78*, *82*). Similarly, the prevalence of microbially bound sediment surfaces (*83*) suggests that the mixed layer may have been entirely to nearly absent in some shallow marine settings during the first ca. 1.5 Myr of the postextinction recovery, and sediment mixing may have been limited for the remainder of the Early Triassic (*78*).

Despite more limited quantitative data, similar patterns of reduced bioturbation are present in strata recording other mass extinctions. Vertical burrows typically reached only 5 cm below the sediment-water interface during the ca. 1 to 1.5 Myr following the end-Triassic mass extinction, before eventually recovering to depths of 15 to 20 cm (*45*, *84*). Mixing intensity was likewise reduced following the end-Triassic extinction, although recovery to preextinction burrow depths and diameters and ichnofabric indices was much more rapid than after the Permian-Triassic extinction (*45*, *84*). As described above, similar patterns appear to have occurred across the Late Devonian biotic crises. Vertical mixing in preextinction Frasnian carbonate platform deposits of the western United States is characterized by average uncorrected burrow depths of ca. 8 cm, whereas postextinction Famennian deposits in this region show almost no vertical burrowing. Bioturbation and vertical mixing return to more robust levels in Mississippian strata in these successions, with depths of burrowing commonly exceeding 10 cm and reaching more than 30 cm in some strata (*43*). In the lower Tournaisian of the Anti-Atlas of Morocco, bioglyphic preservation of *Cruziana reticulata* assemblages record the resurgence of early Paleozoic–style firmground conditions linked to poorly developed sediment mixing in the wake of the Hangenberg Event (*85*). The same is likely true for the end-Cretaceous mass extinction; basal postextinction Paleocene strata are characterized by limited bioturbation (*86*), though sediment mixing appears to have relatively rapidly resumed and achieved preextinction intensities and depths (*87*, *88*). Data spanning the Late Ordovician mass extinction are particularly sparse, though Welsh Basin strata suggest that sediment-mixing intensities were low leading up to and through the extinction interval and do not appear to strongly correlate to extinction pulses recorded in body-fossil records (*89*).

Paleoenvironmental patterns in bioturbation

Nearshore records of bioturbation

The history of bioturbation in high-energy nearshore (e.g., beach and upper shoreface or littoral) settings has followed a distinctive trajectory that appears, to some extent, to have been decoupled from that of shallow subtidal settings. Deep burrows, such as *Skolithos* ichnofabrics penetrating tens of centimeters to a meter into the sediment, appeared by the early Cambrian (*63*), at a time when few burrows in shallow subtidal habitats penetrated more than 5 to 10 cm. However, recent reassessment of classic piperock-bearing units, such as the lower Cambrian Zabriskie Quartzite of the western United States, suggests that the relative abundance of deep *Skolithos* and true piperock of ii 4 to 5 is low, even in facies in which *Skolithos* is abundant (*65*). Moreover, dense *Skolithos* assemblages may, in some instances, represent time-averaging of temporally disparate communities (*4*, *64*) and deep burrows of some *Skolithos* ichnospecies may represent composite structures formed by episodic responses of the inhabitant to sediment accumulation; the entire depth of a fossilized burrow may not have been simultaneously or continuously open during the lifetime of the tracemaker.

Nonetheless, although deep burrowing was clearly established as early as the Cambrian, substantial deepening of the nearshore transition layer subsequently occurred during the Middle Triassic through Middle Jurassic (Fig. 7 and fig. S2). As for shallow subtidal settings, this deepening appears to have been associated with a transition from predominantly vertical cylindrical and U-shaped burrows (e.g., *Skolithos* and *Arenicolites*) to open networks (e.g., *Ophiomorpha* and, to a lesser extent, *Thalassinoides*), often extending >1 m deep, that were constructed by crustaceans (Fig. 6). *Skolithos* piperock became less prevalent throughout the Paleozoic (*63*), although cylindrical and U-shaped burrows were still dominant in Triassic littoral settings (*90*). In Jurassic–Cenozoic high-energy (particularly shoreface) shallow marine deposits, *Ophiomorpha* dominated well-sorted sandy sediments, resulting in the formation of monospecific *Ophiomorpha* piperock ichnofabrics analogous to Paleozoic *Skolithos* piperock (*63*). Although less fabric-disruptive than true *Skolithos* piperock (*40*), crustacean burrow networks were likely continuously maintained as open galleries.

Direct evidence for sedimentary mixed layer depths in Phanerozoic nearshore settings is sparse. However, lower Paleozoic strata deposited in nearshore carbonate settings record variable levels of sedimentary fabric disruption. For instance, lower Cambrian through Middle Ordovician nearshore carbonates preserved in western United States successions do not exceed a mean ii of 1.3 (*4*, *10*, *40*). In contrast, Cambrian and Ordovician nearshore sandstones and peritidal carbonates in other regions appear to have been commonly characterized by higher intensities of fabric disruption. For instance, the lower Cambrian Hawke Bay Formation and peritidal carbonates of the Lower Ordovician Boat Harbor Formation in western Newfoundland are characterized by higher, albeit still moderate, intensities of fabric disruption relative to subtidal strata in this succession (mean ii of 2.9 and 2.5, respectively) (*11*). Dense and commonly deep assemblages of the J-shaped, spiraling burrow *Daedalus* have also been recorded from the Lower Ordovician Armorican Quartzite of Portugal in facies inferred to have formed in high-energy shoreface settings (*66*). However, Hawke Bay and Boat Harbor strata characterized by the highest ii values are dominated by *Skolithos* and *Thalassinoides* (*11*). *Skolithos*, *Thalassinoides*, and *Ophiomorpha* are commonly interpreted to have been dwelling structures ("domichnia") and, in the case of *Skolithos*, occupied by stationary suspension-feeders that may have stabilized their burrows with mucus linings (and, in the case of *Ophiomorpha*, with pellets). The ecology of the *Daedalus* tracemaker remains more cryptic; a lack of differentiated infill suggests that a deposit-feeding lifestyle is unlikely. It has been suggested that this organism may have fed on biofilms or relied on wave-mediated pumping of fine-grained organic-rich particles into the seafloor (*66*). However, geochemical, sedimentological, or morphological evidence for these ecologies is limited. *Daedalus* assemblages, which have only been recorded from Ordovician and lower Silurian strata, are also inferred to represent short-lived episodes of seafloor colonization (*66*). Therefore, the activities of the progenitors of these traces are unlikely to have substantially enhanced diffusive sediment mixing or mixed layer development in the nearshore settings recorded by these units (*4*, *32*).

Deep-sea records of bioturbation

Preserved (i.e., unsubducted) deep-sea successions are rare before the Cretaceous and Cenozoic (but see the Supplementary Materials for discussion). Cretaceous deep-sea chalk deposits indicate that contemporaneous abyssal carbonate sediments were completely

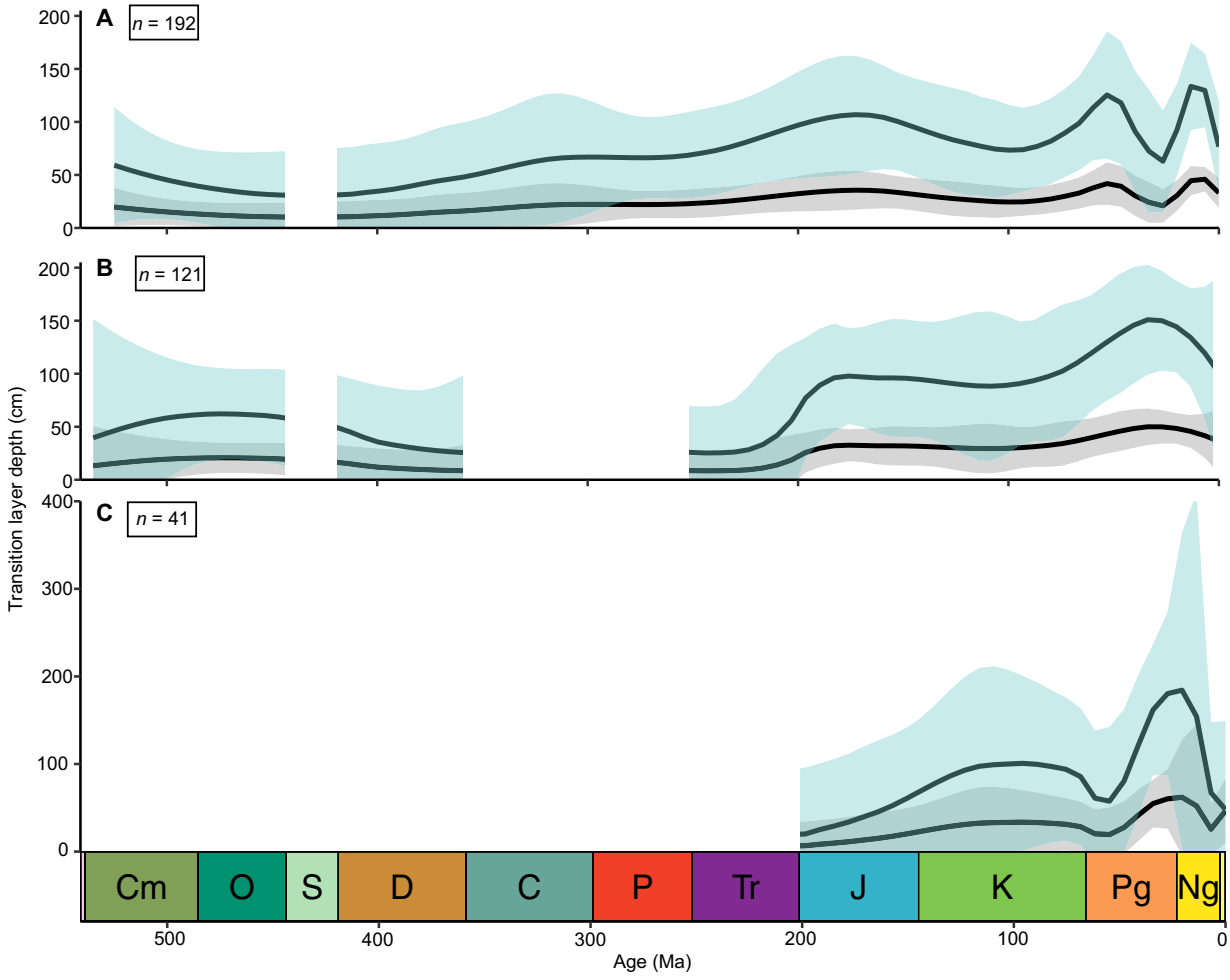

Fig. 7. Transition layer depth over the Phanerozoic in different environments. (**A**) "Nearshore" paleoenvironments, above fair-weather wave base. (**B**) "Shallow" paleoenvironments, between fair-weather and storm wave base. (**C**) "Deep" paleoenvironments, below storm wave base. Gray lower curves reflect data with a lower-bound decompaction factor of 1.0 applied; green upper curves reflect data with an upper-bound decompaction factor of 3.0 applied. Curves produced by LOESS smoothing model with $\alpha = 0.3$. Shaded areas are 95% confidence intervals. Gaps in curves denote systems for which fewer than five observations were recorded. Geological timescale visualized using the R package deeptime (v1.1.1) (*114*).

bioturbated (*58*). Cretaceous deep-sea ichnoassemblages are dominated by deep-tier transition layer burrows; shallow-burrowing structures have been homogenized by intensive sediment mixing (*58*, *87*). Distinct individual trace fossils, where preserved, most commonly overprint previously formed mixed layers and record the activities of "elite" (deep-tier) bioturbators of the transition layer (*2*). Although *Arenicolites* and *Diplocraterion* are common and increase in depth in Mesozoic shallow-water deposits, these ichnotaxa notably decrease in abundance in upper Mesozoic deep-water deposits, whereas *Thalassinoides* abundance and depth increase in deep-water deposits in the Triassic and Jurassic (see the Supplementary Materials for further discussion) (data S2).

In Cenozoic abyssal deep-sea sediments (>1000 m water depth), rates of bioturbation appear to have, under most circumstances, outpaced sediment accumulation rates. To reconstruct intensities of sediment mixing characteristic of the Cenozoic deep-sea record, 48 deep-sea core records collectively spanning the Cenozoic were selected for analysis (data S1). Ichnofabric analysis of these cores indicates that, throughout this interval, deep-sea upper sediments were generally completely bioturbated (ii 5 to 6), such that primary sedimentary structures are not preserved (data S1). As described above, discrete burrows, where present, result from later transition layer overprinting of previously homogenized and buried mixed layer sediments (*86*). In rare cases, physical environmental processes appear to have promoted preservation of vestigial primary sedimentary structures. For instance, Oligocene sediment cores from Atlantic Ocean Drilling Program (ODP) Site 1262 preserve sedimentary evidence of turbidites; bioturbators were unable to completely disturb the lowermost horizons of these event deposits (*91*). Deep-sea sediment cores deposited coevally with the PETM (ODP Sites 690, 1209) show varying intensities of bioturbation. Southern Ocean (ODP Site 690) sediments are moderately to heavily bioturbated throughout this interval (*92*). In cores from the Central Pacific, however, sediments are thoroughly bioturbated below and above the base of the PETM, with relatively limited bioturbation at the recorded onset of the event (*92*, *93*).

Temporal trajectories in the paleoenvironmental distribution of bioturbation

The broad trajectory of the secular trends in deep-tier burrowing described above for shallow subtidal settings is relatively consistent across different marine environments, although the paucity of preserved deep-water Paleozoic successions hampers robust quantification of deep-sea transition layer depths over this interval (see the Supplementary Materials for further discussion). The transition layer appears to have deepened in the early to middle Mesozoic across all marine environmental bins assessed here, although the exact timing of this increase varies by paleoenvironment (Fig. 7 and fig. S2). Nearshore environments experienced the earliest deepening of the transition layer (beginning in the Early to Middle Triassic), followed by shallow subtidal environments in the Late Triassic to Early Jurassic, and deep-water environments lagged notably behind, with transition layer deepening in these settings beginning in the Late Jurassic and near-modern depths not achieved until the Cretaceous (fig. S2). This pattern in transition layer depths follows a classical onshore-offshore model (*94*, *95*), bolstering previous inferences that the evolution of bioturbation follows a similar paleoenvironmental trajectory to other major ecological innovations inferred from body fossil records (*11*, *36*, *96*). Given that the innovations of the MMR may have initiated in shallow marine ecosystems (*55*, *70*), a delayed expansion, during the Cretaceous, of deep burrowing into deep-water sediments may be expected. However, deep-sea transition layers are not well represented in our dataset until the Cenozoic; further exploration of the comparatively sparse Mesozoic deep-sea trace fossil record will be critical to further resolve pre-Cenozoic patterns of transition layer development in continental slope and abyssal settings. Conversely, the only conspicuous divergence in paleoenvironmental patterns of transition layer depth occurred in the Eocene. In both strata recording deep-water environments and those recording nearshore settings, there is a decrease in recorded transition layer depth in this series (Fig. 7). However, this decline is not present in strata recording shallow subtidal environments and only strata recording deep-water environments are characterized by corroborating statistical evidence in the form of a negative changepoint (i.e., a decrease in burrowing depth) (fig. S2).

The history of mixed layer evolution, although currently based on far lower-resolution and patchier records than those available for the transition layer, appears to also follow an onshore-offshore pattern. Shallow subtidal environments may have experienced an earlier escalation in mixed layer depths than at least some nearshore settings, followed substantially later by deep-sea increases in sediment mixing. This pattern has been attributed to onshore-offshore patterns in infaunal activity—and likely onshore-offshore patterns in the emergence and radiation of biological bulldozers—and potentially also to the better oxygenated nature of nearshore and shallow ocean waters located above fair-weather wave base (*11*). Although low background oxygen levels appear to have been characteristic of many marine settings during the early (and potentially later) Paleozoic (*97*), wind- and storm-mediated mixing and thus greater exchange with atmospheric oxygen may have increased the viability of shallow-water settings for the evolutionary expansion of deep and intensive sediment mixing.

DISCUSSION

Coupled evolutionary and environmental patterns in Phanerozoic marine bioturbation

The evolution of the marine sedimentary mixed and transition layers has been decoupled over the Phanerozoic. In shallow subtidal environments, development of a deep mixed layer was notably protracted and may not have reached modern-style depths until the late Mesozoic (data S1). Although direct records of sediment mixed layer depth remain sparse through many intervals of the Phanerozoic, a quantitative assessment of the maximum depths of ichnotaxa commonly associated with deep-tier burrowing provides a critical window into the evolution of the sedimentary transition layer. The deepening of the transition layer substantially preceded the deepening of the mixed layer. Burrows exceeding a meter in depth were excavated in subtidal and nearshore environments as early as the Cambrian, although average deep-tier burrowing remained much shallower through this interval. During the Mesozoic, the transition layer substantially deepened in conjunction with a greater abundance and distribution of deep *Zoophycos* as well as *Arenicolites* and *Diplocraterion* U-shaped burrows; subsequent Cenozoic increases in transition layer depth, particularly in *Ophiomorpha* and *Thalassinoides* burrow networks, may be linked to episodes of warming that although prominent did not exceed infaunal thermal tolerances. Mesozoic increases in the depth of the mixed and transition layers may have been spurred by increases in infaunalization and sediment-mixing rates and depths associated with the MMR, radiations in key bulldozing and deep-tier burrowing taxa, changes in nutrient availability, increases in seawater oxygenation, or some combination thereof. The onshore-offshore environmental shift that characterized the evolution of both the mixed and transition layers mirrors patterns previously noted from marine body fossil records. The higher resolution of the Cenozoic record allows for recognition of additional shifts in transition layer depth; determination of the environmental and evolutionary triggers that led to these increases requires further study.

Ecological and biogeochemical implications of Phanerozoic developments in the mixed and transition layers

The protracted development of the mixed layer over the Phanerozoic has important implications for interpretations of the paleoecological and biogeochemical evolution of seafloor environments and for the timing of the emergence of bioturbating animals as ecosystem engineers. The temporal lag between the advent of infaunalization and the development of intensively mixed sediments suggests, in contrast to the historical view, that earliest Phanerozoic bioturbators were not efficient "engineers" in the sense of modern marine bioturbators.

Studies that have implemented field-based bioturbation data into biogeochemical models indicate that earliest Paleozoic sediment-mixing animals, unlike their younger counterparts, likely did not mediate substantial increases in seafloor oxygenation (*98*), sulfide reoxidation (*35*) [but see (*99*)], or phosphorus burial (*100*), in contrast to previous suggestions (*101*). These delays in the emergence of widespread deeper sediment mixing and associated biogeochemical "engineering" were presumably not due to lack of appropriate physiology, as bilaterian infauna appeared by the late Ediacaran [e.g., (*20*)], and biomineralizing and relatively large infauna appeared by Cambrian Age 3. Moreover, lower Cambrian successions contain trace fossils attributed to mobile deposit-feeders, suggesting that at least some early Cambrian infauna had the ability to mix sediments (*4*). These lags may instead indicate delays in the ecological implementation of efficient sediment-mixing behaviors used by modern "keystone" bioturbators, such as biological bulldozing [compare to (*52*)]. Early Paleozoic infauna, in particular, may have lacked

sufficient nutritional incentives or energy resources (particularly under the low-oxygen bottom waters prevalent in early Paleozoic oceans) to pursue metabolically costly activities such as deep and intensive biological bulldozing on an ecologically or environmentally widespread scale (*4*, *11*). For instance, nutritional incentives for deep sediment mixing may have been comparatively low if surface ocean-produced organic matter was more efficiently exported to the seafloor surface under lower seawater oxygen levels. The radiation of biological bulldozers, potentially initiating in the middle to late Paleozoic and continuing into the Mesozoic, may be partly tied to coeval increases in atmospheric and marine oxygen levels—perhaps in turn linked to either the terrestrial radiation of arboreal vascular plants and associated changes in continental nutrient fluxes (*102*) or changes in export productivity (*71*), and an associated lessening of metabolic constraints on bioturbation (*4*).

Increases in the depth of the transition layer would have also substantially shaped seafloor biogeochemistry and habitability, particularly by increasing the volume of sediment exposed to ocean bottom waters. Many modern vertical burrows are either passively or actively ventilated through the activities of their occupants; this bioirrigation enhances the flux of solutes between bottom waters and sedimentary pore waters (*103*). These effects may extend far beyond the area immediately surrounding burrow walls, especially in the presence of large and/or powerful bioirrigating taxa (*104*). Greater depths or intensities of bioirrigation associated with deepening of the transition layer would likely have increased remineralization of organic carbon (*105*). On ecologic timescales, these activities may also have increased local oxygen bioavailability in upper seafloor sediments but, on geologic timescales, decreased oxygen supply via negative feedbacks between marine organic carbon burial and atmospheric oxygen accumulation (*106*). Even if burrows were not actively ventilated, increasing burrow depth would have resulted in a deeper oxic zone, as recently demonstrated by a diagenetic modeling study, which found that deeper-penetrating *Skolithos* burrows oxygenate a substantially larger volume of sediments than shallower burrows (*65*). Therefore, as larger, deeper burrows became more common in the Mesozoic and Cenozoic, increased depths of seafloor oxidation should have driven higher organic carbon remineralization rates. Increases in bioirrigation associated with deepening of the transition layer may have also decreased the burial fluxes of other reductants, such as ferrous iron and hydrogen sulfide (*107*)—though recent work has highlighted that burrow density as well as burrow depth may strongly shape extents of sulfide reoxidation (*65*). Greater bioirrigation depths should have also mediated decreases in phosphorus burial, fostering more extensive nutrient regeneration (*100*), which may, in turn, have spurred further increases in productivity and organismal biomass associated with episodes such as the MMR.

The eventual emergence of deep and intensive sediment mixing may have also markedly affected the ecology of benthic ecosystems. Shallow bioturbation has been proposed to have contributed to the widespread development of authigenic hardgrounds in the Ordovician, thereby contributing to the Great Ordovician Biodiversification Event (*108*). The radiation of deep-burrowing mollusks, crustaceans, and worms appears to have played a pivotal role in driving the ecological arms race of the MMR. Mesozoic changes to the biological pump (*71*) may, in turn, have fostered the late Mesozoic and Cenozoic intensification of deep-sea sediment mixing. Shallow marine environments appear to have been at the forefront of increases in sediment-mixing intensity and both shallow subtidal and nearshore environments experienced early deepening of the transition layer; the evolution of bioturbation, like other evolutionary phenomena, appears to have largely followed an onshore-offshore trend. Modern shallow marine sediments are also foci of intensive and dynamic biogeochemical cycling and thus the eventual rise of widespread deep burrowing and sediment-mixing behaviors in these settings was likely critical to the establishment of modern-style biogeochemical cycling.

Future directions for Phanerozoic bioturbation research

Mixed and transition layer records nonetheless retain considerable gaps that mandate further study. Mixed layer records, with the exception of certain intervals such as the lower Paleozoic, remain substantially scarcer, lower in resolution, and patchier than transition layer datasets; collection of higher-resolution and stratigraphically constrained sediment-mixing data will be essential to ground truth and quantify our proposed mixed layer trajectory. Of particular concern is the paucity of data from uppermost lower and middle Paleozoic strata for either sediment mixing or deep burrowing. This is an interval for which body fossil and biogeochemical archives record major evolutionary transitions that may have affected infaunal communities, including the expansion of land plants and the Late Devonian biotic crises. In addition, ichnological characterization of deep-tier burrowing through the Middle and Late Triassic and sediment-mixing records through the Late Triassic and Jurassic remain sparse, particularly in comparison to data available for the postextinction recovery interval of the Early Triassic. Further investigation of these and other intervals may therefore lend critical insights into both ecological and biogeochemical consequences of changes in burrowing intensity, depth, or style.

MATERIALS AND METHODS

Mixed layer assessment

There is no single proxy that provides a direct correlation for the depth of the sedimentary mixed layer recorded in geologic successions. However, a range of sedimentological and ichnological properties—particularly those that record information on intensities of sedimentary fabric disruption and rheological conditions in the vicinity of the paleo-sediment–water interface—can, when integrated, provide critical quantitative, semiquantitative, and descriptive data from which sediment-mixing intensities and depths can be interpreted. These proxies are summarized and discussed in detail in (*4*). Here, we briefly summarize those proxies upon which we chiefly relied, as discussed in the main text, to estimate extents of seafloor sediment mixing through the Phanerozoic, based on all discoverable relevant papers and dissertations in the English-language scientific literature, and in several cases supplemented by first-hand observation of International Ocean Discovery Program (IODP) and ODP deep marine sediment cores and core images (see the Supplementary Materials and data S1). Both these data and our transition layer dataset (see below) are global in scope though, like many paleontological databases, contributions from Asia, Europe, and North America are relatively more abundant, and data from Africa, Antarctica, South America, and, to varying extents, Oceania are comparatively underrepresented. We consider expanding not only the abundance of mixed layer data but also the geographic scope of these data and the inclusion of data from papers published in languages other than English

to all be important priorities for future studies of Phanerozoic bioturbation.

1) The Ichnofabric Index (ii) (*34*) schematically characterizes sedimentary fabrics along a scale ranging from undisrupted physical stratification (ii 1) to depositional fabrics fully overprinted by burrowing (ii 5) to fully homogenized and texturally massive (ii 6). As sediments accumulate and the sediments previously adjacent to the sediment-water interface are advected downward, true mixed layers (ii 6) may be subsequently overprinted by deep burrowing associated with younger transition layers; in our descriptions, we have noted instances in which ichnofabrics are interpreted to represent palimpsests of older mixed layers and younger transition layers.

2) Event bed thickness provides another window into mixing depths and intensities (*36*, *39*). Although hydrodynamic energy and flow character, grain size, and seabed roughness will dictate the scale of event bed (e.g., sandstone tempestite) deposition, postdepositional bioturbation will determine whether depositional events are preserved as discrete beds or whether these are merged with adjacent beds due to sediment remobilization by bioturbators. Through this process of postdepositional transport of sediments and overprinting of bed junctions, bioturbation commonly "erases" the thinnest event beds by blending them with adjacent bedforms. Therefore, the coherency and the minimum and mean thickness of event beds are commonly proportional to rates and depths of sediment mixing.

3) The fidelity of preservation of trace fossils, particularly structures formed proximal to the paleo-sediment–water interface, correlates directly to the rheology of seafloor sediments and is indicative of whether they were hydroplastic and firm and thus poorly bioturbated, or soupy and thus well bioturbated (*33*). The presence of "bioglyphs" (*109*) or crisply preserved organismal "fingerprints," such as scratch marks along arthropod-produced surficial traces or shallow-tier burrows, is indicative of poorly mixed sediments at the depth of trace excavation.

4) Similarly, the presence of sole marks, particularly small-scale and crisply preserved features like tool marks and flute casts, is a direct indicator of firm and poorly bioturbated seafloor sediments at the time and depth of emplacement (*4*).

5) The depth of trace fossils typically formed at or connected to the sediment-water interface and extents to which these are erosionally truncated can provide further information regarding both maximum depths of seafloor colonization and the distance of trace fossil assemblages or other paleo-rheological sedimentary indicators from the paleo-sediment–water interface.

6) The paleobiological and paleoecological complexity of trace fossil assemblages, including trace fossil size, density, architectural complexity, and disparity, can provide critical insights into extents of both horizontal and vertical infaunalization, decipher tiering relationships, and reconstruct successive episodes of seafloor colonization (*110*). These data, in turn, provide critical context for reconstructing the respective depths of the mixed and transition layers and thus, like proxies 4 and 5, facilitate assessment of depth of emplacement relative to the paleo-sediment–water interface.

Transition layer dataset compilation

Our dataset was compiled from 213 English-language papers and comprises burrow depth measurements for six ichnotaxa: *Arenicolites*, *Diplocraterion*, *Ophiomorpha*, *Skolithos*, *Thalassinoides*, and *Zoophycos* (see examples of each of these trace fossils in Fig. 2). These ichnotaxa were selected because they are relatively common, have long stratigraphic ranges (with the exception of *Ophiomorpha*, the first occurrence of each ichnotaxon is in the Paleozoic), are vertical or near-vertical in orientation, and are classically considered to be among the deepest burrows in the fossil record. Papers were sourced via Google Scholar searches using the following search term structure: "[ichnotaxon name] AND (depth* OR length* OR penetration)". More than a thousand papers were surveyed to identify the sources for our dataset. Only papers reporting the vertical extent of sediment penetration for at least one of the six selected ichnotaxa were used in compiling this dataset. The maximum burrow depth reported for each selected ichnotaxon appearing in a sedimentary unit was extracted and used to build the dataset (e.g., if *Arenicolites* in a particular unit were reported as having a penetration depth of 3 to 8 cm, the depth recorded in our database for that unit would be 8 cm); this is because the depth of the transition layer at a given time is equal to the depth of the deepest-penetrating occupied burrow structure (*2*).

A total of 390 marine burrow measurements are included in our dataset, representing at least 260 sedimentary units and 18 modern localities or sediment cores. In addition to burrow depth (in centimeters), numerous other parameters were collected for each burrow (data S2). These include the name and location of each stratigraphic unit, the age of the unit, and paleoenvironmental interpretations, as available. Where absolute numeric ages were not provided, the midpoint of the most precise age division given by the source was used as the estimated age of the burrow, with midpoints calculated based on the International Chronostratigraphic Chart. Burrows for which a range of chronostratigraphic units was provided are binned with the uppermost of these chronostratigraphic units for erathem-, system-, and series-level analyses. The resulting dataset spans the entire Phanerozoic (the oldest burrow in the dataset is Fortunian in age, the youngest are from modern sediments) and represents a wide range of marine environments.

Only trace fossils found in marine environments and lithofacies were considered for this analysis. Paleoenvironments above fair-weather wave base were classified as nearshore (shoreface, estuary, lagoon, intertidal, etc.); those below fair-weather wave base but above storm wave base were classified as shallow subtidal (including upper offshore and inner shelf environments); and those below storm wave base were classified as deep (outer shelf, continental slope, and abyssal environments).

Transition layer analyses

If key environmental stressors were noted by the authors (particularly oxygen stress, occasional or persistent subaerial exposure, and/or brackish conditions), these occurrences were flagged as potentially reflecting burrowing under stressed conditions that may not have been representative of coeval "background," normal marine conditions. Removal of these data did not affect trends in burrow depth. Similarly, all analyses were performed both with and without burrows recorded in units deposited during or immediately following any of the Big Five mass extinction events (Late Ordovician, Late Devonian, Permian–Triassic, end-Triassic, and end-Cretaceous); removal of these mass extinction–associated records did not affect overall trends in Phanerozoic transition layer depth, although Lower Triassic bins are substantially less populated when burrows measured in studies of the Permian–Triassic mass extinction and subsequent recovery are removed.

Traces in both lithified rock and unconsolidated marine sediment are included in this dataset. A total of 25 burrows in our dataset

come from unconsolidated sediments. These were mostly measured in modern coastal environments, although nine were burrows measured in sediment cores sampled by various ocean drilling projects (age range: Eocene to Quaternary). For the 365 burrows found in lithified sediments, precompaction burrow depth was estimated using a lower-bound decompaction factor of 1.0 and an upper-bound decompaction factor of 3.0. Most decompaction factors for common sedimentary lithologies fall within these ranges (*111*, *112*). A standard LOESS smoothing regression was performed on both the upper and lower bounds of burrow depths produced by application of these decompaction factors to estimate transition layer depths across the Phanerozoic.

To estimate a single transition layer depth representative of each sedimentary unit in our database, a normalized dataset was produced by retaining only the deepest burrow measurement from a single horizon, bed, member, or formation; the highest resolution available was used in each case. To consider our transition layer depths under an infaunal tiering framework, we adapted the burrow tiering classification scheme of Bottjer and Ausich (*14*) and classified each resulting transition layer datum as "shallow" (<6 cm), "intermediate" (6 to 12 cm), or "deep" (>12 cm).

All transition layer depths produced using the normalization scheme described above were used for changepoint analyses except for those that relied on unconsolidated burrow measurements; this was done so that the original depth measurements of lithified burrows, rather than the depth range produced by application of decompaction factors, could be quantitatively assessed. For these changepoint analyses, all transition layer depths were placed consecutively in chronologic order with a null model of uniform distribution, such that the leftmost value on the x axis corresponds to the oldest burrow in the dataset and the rightmost value corresponds to the youngest burrow. If more than one burrow depth was reported by the same authors from a single interval within a stratigraphic unit, only the deepest measurement from that interval was used to more accurately reflect the true maximum extent of the sedimentary transition layer. Changepoint analyses were performed using the PAST software package (*113*). One million simulations were run with a permitted maximum of 10 detectable changepoints; the number of changepoints was unrestricted below this maximum. Changepoints were recognized where the average changepoint model identified >10% increase or decrease in burrow or transition layer depth and for which an elevated percentage of model simulations converged in identifying changepoints in a given part of the dataset (i.e., more than three times the mean of the 20 preceding data points).

Supplementary Materials

The PDF file includes:
Supplementary Discussion
Figs. S1 to S3
Legends for data S1 and S2
References

Other Supplementary Material for this manuscript includes the following:
Data S1 and S2

REFERENCES AND NOTES

1. B. P. Boudreau, Mean mixed depth of sediments: The wherefore and the why. *Limnol. Oceanogr.* **43**, 524–526 (1998).
2. A. A. Ekdale, L. N. Muller, M. T. Novak, Quantitative ichnology of modern pelagic deposits in the abyssal Atlantic. *Palaeogeogr. Palaeoclimatol. Palaeoecol.* **45**, 189–223 (1984).
3. S. Zhang, M. Solan, L. Tarhan, Global distribution and environmental correlates of marine bioturbation. *Curr. Biol.* **34**, 2580–2593.e4 (2024).
4. L. G. Tarhan, The early Paleozoic development of bioturbation: Evolutionary and geobiological consequences. *Earth Sci. Rev.* **178**, 177–207 (2018).
5. F. J. R. Meysman, J. J. Middelburg, C. H. R. Heip, Bioturbation: A fresh look at Darwin's last idea. *Trends Ecol. Evol.* **21**, 688–695 (2006).
6. S. M. Awramik, Precambrian columnar stromatolite diversity: Reflection of metazoan appearance. *Science* **174**, 825–827 (1971).
7. R. A. Boyle, T. W. Dahl, A. W. Dale, G. A. Shields-Zhou, M. Zhu, M. D. Brasier, D. E. Canfield, T. M. Lenton, Stabilization of the coupled oxygen and phosphorus cycles by the evolution of bioturbation. *Nat. Geosci.* **7**, 671–676 (2014).
8. M. Laflamme, S. A. F. Darroch, S. M. Tweedt, K. J. Peterson, D. H. Erwin, The end of the Ediacara biota: Extinction, biotic replacement, or Cheshire Cat? *Gondw. Res.* **23**, 558–573 (2013).
9. J. D. Howard, H. E. Reineck, Depositional facies of high-energy beach-to-offshore sequence: Comparison with low-energy sequence. *AAPG Bull.* **65**, 807–830 (1981).
10. M. L. Droser, D. J. Bottjer, Trends in depth and extent of bioturbation in Cambrian carbonate marine environments, western United States. *Geology* **16**, 233–236 (1988).
11. L. G. Tarhan, R. Z. Nolan, S. Westacott, J. O. Shaw, S. B. Pruss, Environmental and temporal patterns in bioturbation in the Cambrian-Ordovician of Western Newfoundland. *Geobiology* **21**, 571–591 (2023).
12. W. I. Ausich, D. J. Bottjer, Tiering in suspension-feeding communities on soft substrata throughout the Phanerozoic. *Science* **216**, 173–174 (1982).
13. W. I. Ausich, D. J. Bottjer, "Epifaunal and infaunal interactions," in *Palaeobiology II*, D. E. G. Briggs, P. R. Crowther, Eds. (Blackwell, 2001), pp. 384–386.
14. D. J. Bottjer, W. I. Ausich, Phanerozoic development of tiering in soft substrata suspension-feeding communities. *Paleobiology* **12**, 400–420 (1986).
15. A. G. Liu, D. Mcilroy, J. J. Matthews, M. D. Brasier, Confirming the metazoan character of a 565 Ma trace-fossil assemblage from Mistaken Point, Newfoundland. *Palaios* **29**, 420–430 (2014).
16. M. L. Droser, L. G. Tarhan, J. G. Gehling, The rise of animals in a changing environment: Global ecological innovation in the late Ediacaran. *Annu. Rev. Earth Planet. Sci.* **45**, 593–617 (2017).
17. C. Carbone, G. M. Narbonne, When life got smart: The evolution of behavioral complexity through the Ediacaran and early Cambrian of NW Canada. *J. Paleo.* **88**, 309–330 (2014).
18. S. Jensen, M. L. Droser, J. G. Gehling, "A critical look at the Ediacaran trace fossil record," in *Neoproterozoic Geobiology and Paleobiology*, S. Xiao, A. J. Kaufman, Eds. (Springer, 2006), chap. 5, pp. 115–157.
19. A. Seilacher, Biomat-related lifestyles in the Precambrian. *Palaios* **14**, 86–93 (1999).
20. Z. Chen, C. M. Zhou, M. Meyer, K. Xiang, J. D. Schiffbauer, X. L. Yuan, S. H. Xiao, Trace fossil evidence for Ediacaran bilaterian animals with complex behaviors. *Precambrian Res.* **224**, 690–701 (2013).
21. G. R. O'Neil, L. S. Tackett, M. B. Meyer, The role of surficial bioturbation in the latest Ediacaran: A quantitative analysis of trace fossil intensity in the terminal Ediacaran-lower Cambrian of California. *Palaios* **37**, 703–717 (2022).
22. S. A. F. Darroch, T. H. Boag, R. A. Racicot, S. Tweedt, S. J. Mason, D. H. Erwin, M. Laflamme, A mixed Ediacaran-metazoan assemblage from the Zaris Sub-basin, Namibia. *Palaeogeogr. Palaeoclimatol. Palaeoecol.* **459**, 198–208 (2016).
23. S. Jensen, B. N. Runnegar, A complex trace fossil from the Spitskop Member (terminal Ediacaran-? Lower Cambrian) of southern Namibia. *Geol. Mag.* **142**, 561–569 (2005).
24. L. G. Tarhan, P. M. Myrow, E. F. Smith, L. L. Nelson, P. M. Sadler, Infaunal augurs of the Cambrian explosion: An Ediacaran trace fossil assemblage from Nevada, USA. *Geobiology* **18**, 486–496 (2020).
25. B. Runnegar, J. G. Gehling, S. Jensen, M. R. Saltzman, Ediacaran paleobiology and biostratigraphy of the Nama Group, Namibia, with emphasis on the erniettomorphs, tubular and trace fossils, and a new sponge, *Arimasia germsi* n. gen. n. sp. *J. Paleontol.* **98**, 1–59 (2024).
26. L. A. Buatois, J. Almond, M. G. Mángano, S. Jensen, G. J. B. Germs, Sediment disturbance by Ediacaran bulldozers and the roots of the Cambrian explosion. *Sci. Rep.* **8**, 4514 (2018).
27. L. A. Parry, P. C. Boggiani, D. J. Condon, R. J. Garwood, J. D. M. Leme, D. McIlroy, M. D. Brasier, R. Trindade, G. A. C. Campanha, M. L. A. F. Pacheco, C. Q. C. Diniz, A. G. Liu, Ichnological evidence for meiofaunal bilaterians from the terminal Ediacaran and earliest Cambrian of Brazil. *Nat. Ecol. Evol.* **1**, 1455–1464 (2017).
28. T. P. Crimes, Changes in the trace fossil biota across the Proterozoic-Phanerozoic boundary. *J. Geol. Soc. London* **149**, 637–646 (1992).
29. D. J. Bottjer, J. W. Hagadorn, S. Q. Dornbos, The Cambrian substrate revolution. *GSA Today* **10**, 1–7 (2000).
30. A. Seilacher, F. Pflüger, "From biomats to benthic agriculture: A biohistoric revolution," in *Biostabilization of Sediments*, W. E. Krumbein, D. M. Paterson, L. J. Stal, Eds. (Bibliotheks and Informationssystem der Carl von Ossietzky Universität, 1994), pp. 97–105.
31. L. G. Herringshaw, R. H. T. Callow, D. McIlroy, "Engineering the Cambrian explosion: The earliest bioturbators as ecosystem engineers," in *Earth System Evolution and Early Life: A*

Celebration of the Work of Martin Brasier, A. T. Brasier, D. McIlroy, N. McLoughlin, Eds. (The Geological Society of London, 2017), vol. 448, pp. 369–382.
32. M. L. Droser, S. Jensen, J. G. Gehling, Trace fossils and substrates of the terminal Proterozoic-Cambrian transition: Implications for the record of early bilaterians and sediment mixing. *Proc. Natl. Acad. Sci. U.S.A.* **99**, 12572–12576 (2002).
33. L. G. Tarhan, M. L. Droser, Widespread delayed mixing in early to middle Cambrian marine shelfal settings. *Palaeogeogr. Palaeoclimatol. Palaeoecol.* **399**, 310–322 (2014).
34. M. L. Droser, D. J. Bottjer, A semiquantitative field classification of ichnofabric. *J. Sediment. Petrol.* **56**, 558–559 (1986).
35. L. G. Tarhan, M. L. Droser, N. J. Planavsky, D. T. Johnston, Protracted development of bioturbation through the early Palaeozoic Era. *Nat. Geosci.* **8**, 865–869 (2015).
36. J. J. Sepkoski, Jr., R. K. Bambach, M. L. Droser, "Secular changes in Phanerozoic event bedding and the biological overprint," in *Cycles and Events in Stratigraphy*, G. Einsele, W. Ricken, A. Seilacher, Eds. (Springer Verlag, 1991), pp. 298–312.
37. D. Fillion, R. K. Pickerill, Ichnology of the Upper Cambrian? to Lower Ordovician Bell Island and Wabana groups of eastern Newfoundland, Canada. *Palaeontographica Canadiana* **7**, 1–83 (1990).
38. R. W. Frey, T. M. Chowns, "Trace fossils from the Ringgold road cut (Ordovician and Silurian), Georgia," in *Sedimentary Environments in the Paleozoic Rocks of Northwest Georgia* (Georgia Geological Society, 1972), pp. 45–100.
39. D. W. Larson, D. C. Rhoads, "The evolution of infaunal communities and sedimentary fabrics," in *Biotic Interaction in Recent and Fossil Benthic Communities*, M. J. S. Tevesz, Ed. (Springer, 1983), pp. 627–648.
40. M. L. Droser, D. J. Bottjer, Ordovician increase in extent and depth of bioturbation: Implications for understanding early Paleozoic ecospace utilization. *Geology* **17**, 850–852 (1989).
41. M. Bendella, M. Benyoucef, R. Mikuláš, I. Bouchemla, B. Ferré, Storm-dominated shallow marine trace fossils of the Lower Devonian Teferguenite Formation (Saoura valley, Algeria). *Ital. J. Geosci.* **141**, 400–425 (2022).
42. A. Draoui, M. Bendella, B. Ferré, M. Benzina, M. Zaagane, K. Ziouit, A. Boutadaraa, A. Boutadaraa, A. Salah, Trace fossil assemblages from the Lower Devonian (Lochkovian-Emsian) of the Touat area (Reggane Basin, Algerian Sahara) and their palaeoenvironmental significance. *Palaeobiodivers. Palaeoenviron.* **104**, 275–303 (2024).
43. W. T. Phelps, "Ecologic changes associated with the Late Devonian mass extinction: Evidence from the Great Basin and Rocky Mountain regions, western United States", thesis, University of California, Riverside (2007).
44. M. Luo, G. R. Shi, First record of the trace fossil Protovirgularia from the Middle Permian of southeastern Gondwana (southern Sydney Basin, Australia). *Alcheringa* **41**, 335–349 (2017).
45. R. J. Twitchett, C. Barras, "Trace fossils in the aftermath of mass extinction events," in *The Application of Ichnology to Palaeoenvironmental and Stratigraphic Analysis*, D. McIlroy, Ed. (The Geological Society of London, 2004), vol. 228, pp. 397–418.
46. K. J. Whidden, D. J. Bottjer, in *Cavalcade of Carbonates* (Pacific Section, SEPM, 1989), pp. 121–125.
47. R. J. Twitchett, P. B. Wignall, Trace fossils and the aftermath of the Permo-Triassic mass extinction: Evidence from northern Italy. *Palaeogeogr. Palaeoclimatol. Palaeoecol.* **124**, 137–151 (1996).
48. X. Q. Feng, Z.-Q. Chen, D. J. Bottjer, M. L. Fraiser, Y. Xu, M. Lu, Additional records of ichnogenus *Rhizocorallium* from the Lower and Middle Triassic, South China: Implications for biotic recovery after the end-Permian mass extinction. *Geol. Soc. Am. Bull.* **130**, 1197–1215 (2018).
49. D. S. Brandt, Preservation of event beds through time. *Palaios* **1**, 92–96 (1986).
50. L. A. Buatois, N. B. Carmona, H. A. Curran, R. G. Netto, M. G. Mangano, A. Wetzel, "The Mesozoic marine revolution," in *Trace-Fossil Record of Major Evolutionary Events, Vol 2: Mesozoic and Cenozoic*, M. G. Mangano, L. A. Buatois, Eds. (Springer, 2016), pp. 19–134.
51. L. S. Tackett, D. J. Bottjer, Faunal succession of Norian (Late Triassic) level-bottom benthos in the Lombardian Basin: Implications for the timing, rate, and nature of the early Mesozoic Marine Revolution. *Palaios* **27**, 585–593 (2012).
52. C. W. Thayer, "Sediment-mediated biological disturbance and the evolution of marine benthos," in *Biotic Interactions in Recent and Fossil Benthic Communities*, M. J. S. Tevesz, P. L. McCall, Eds. (Plenum Press, 1983), pp. 480–595.
53. R. K. Bambach, "Ecospace utilization and guilds in marine communities through the Phanerozoic," in *Biotic Interactions in Recent and Fossil Benthic Communities*, M. J. S. Tevesz, P. L. McCall, Eds. (Springer, 1983), chap. 15, pp. 719–746.
54. J. J. Sepkoski Jr., A factor analytic description of the Phanerozoic marine fossil record. *Paleobiology* **7**, 36–53 (1981).
55. G. J. Vermeij, The Mesozoic marine revolution: Evidence from snails, predators and grazers. *Paleobiology* **3**, 245–258 (1977).
56. C. E. Savrda, D. J. Bottjer, Trace-fossil model for reconstructing oxygenation histories of ancient marine bottom waters: Application to Upper Cretaceous Niobrara Formation, Colorado. *Palaeogeogr. Palaeoclimatol. Palaeoecol.* **74**, 49–74 (1989).
57. D. J. Bottjer, "Paleoecology, ichnology, and depositional environments of Upper Cretaceous chalks (Anona Formation; chalk member of Saratoga Formation), southwestern Arkansas," thesis, Indiana University, Bloomington, IN (1979).
58. A. A. Ekdale, R. G. Bromley, Comparative ichnology of shelf-sea and deep-sea chalk. *J. Paleo.* **58**, 322–332 (1984).
59. M. Manojlovic, M. E. Clapham, The role of bioturbation-driven substrate disturbance in the Mesozoic brachiopod decline. *Paleobiology* **47**, 86–100 (2021).
60. M. Clapham, I. Xia, J. Cai, M. Manojlovic, S. Peters, paper presented at the North American Paleontological Convention, 2019.
61. M. J. Nicolo, G. R. Dickens, C. J. Hollis, South Pacific intermediate water oxygen depletion at the onset of the Paleocene-Eocene thermal maximum as depicted in New Zealand margin sections. *Paleoceanography* **25**, PA4210 (2010).
62. P. Stassen, E. Thomas, R. P. Speijer, Integrated stratigraphy of the Paleocene-Eocene thermal maximum in the New Jersey Coastal Plain: Toward understanding the effects of global warming in a shelf environment. *Paleoceanography* **27**, PA4210 (2012).
63. M. L. Droser, Ichnofabric of the Paleozoic *Skolithos* ichnofacies and the nature and distribution of *Skolithos* piperock. *Palaios* **6**, 316–325 (1991).
64. D. McIlroy, M. Garton, Realistic interpretation of ichnofabrics and palaeoecology of the pipe-rock biotope. *Lethaia* **43**, 420–426 (2010).
65. S. Westacott, M. Y. Zhao, L. G. Tarhan, Extent and biogeochemical impact of *Skolithos* piperock in the lower Cambrian Zabriskie Quartzite (California, USA). *Palaeogeogr. Palaeoclimatol. Palaeoecol.* **651**, 112381 (2024).
66. C. Neto de Carvalho, A. Baucon, D. Gonçalves, *Daedalus* mega-ichnosite from the Muradal Mountain (Naturtejo Global Geopark, Central Portugal): Between the Agronomic Revolution and the Ordovician Radiation. *Comunic. Geol.* **103**, 59–70 (2016).
67. E. M. Harper, "The Mesozoic Marine Revolution," in *Predator-Prey Interactions in the Fossil Record*, P. H. Kelley, M. Kowalewski, T. A. Hansen, Eds. (Kluwer Academic/Plenum Publishers, 2003), chap. 18, pp. 433–455.
68. C. E. Schweitzer, R. M. Feldmann, Faunal turnover and niche stability in marine Decapoda in the Phanerozoic. *J. Crustac. Biol.* **35**, 633–649 (2015).
69. M. G. Mángano, L. A. Buatois, N. J. Minter, R. Gougeon, Bioturbators as ecosystem engineers in space and time. *Palaeontology* **67**, e12732 (2024).
70. G. J. Vermeij, *Evolution and Escalation: An Ecological History of Life* (Princeton Univ. Press, 1987).
71. A. H. Knoll, M. J. Follows, A bottom-up perspective on ecosystem change in Mesozoic oceans. *Proc. R. Soc. B or Proc. Biol. Sci.* **283**, 20161755 (2016).
72. W. Y. Lu, A. Ridgwell, E. Thomas, D. S. Hardisty, G. Luo, T. J. Algeo, M. R. Saltzman, B. C. Gill, Y. N. Shen, H. F. Ling, C. T. Edwards, M. T. Whalen, X. L. Zhou, K. M. Gutchess, L. Jin, R. E. M. Rickaby, H. C. Jenkyns, T. W. Lyons, T. M. Lenton, L. R. Kump, Z. L. Lu, Late inception of a resiliently oxygenated upper ocean. *Science* **361**, 174–177 (2018).
73. R. Przeslawski, Q. Zhu, R. Aller, Effects of abiotic stressors on infaunal burrowing and associated sediment characteristics. *Mar. Ecol. Prog. Ser.* **392**, 33–42 (2009).
74. Z. Q. Zhou, T. J. Bouma, G. S. Fivash, T. Ysebaert, L. van IJzerloo, J. van Dalen, B. van Dam, B. Walles, Thermal stress affects bioturbators' burrowing behavior: A mesocosm experiment on common cockles (*Cerastoderma edule*). *Sci. Total Environ.* **824**, 153621 (2022).
75. R. H. B. Fraaije, Evolution of reef-associated decapod crustaceans through time, with particular reference to the Maastrichtian type area. *Contrib. Zool.* **72**, 119–130 (2003).
76. C. E. Schweitzer, Paleobiogeography of Cretaceous and Tertiary decapod crustaceans of the North Pacific Ocean. *J. Paleo.* **75**, 808–826 (2001).
77. N. B. Carmona, L. A. Buatois, M. G. Mángano, The trace fossil record of burrowing decapod crustaceans: Evaluating evolutionary radiations and behavioural convergence. *Foss. Strata* **51**, 141–153 (2004).
78. R. Hofmann, L. A. Buatois, R. B. MacNaughton, M. G. Mángano, Loss of the sedimentary mixed layer as a result of the end-Permian extinction. *Palaeogeogr. Palaeoclimatol. Palaeoecol.* **428**, 1–11 (2015).
79. X. Q. Feng, Z. Q. Chen, A. Woods, Y. Pei, S. Q. Wu, Y. H. Fang, M. Luo, Y. L. Xu, Anisian (Middle Triassic) marine ichnocoenoses from the eastern and western margins of the Kamdian Continent, Yunnan Province, SW China: Implications for the Triassic biotic recovery. *Global Planet. Change* **157**, 194–213 (2017).
80. T. W. Beatty, J. P. Zonneveld, C. M. Henderson, Anomalously diverse Early Triassic ichnofossil assemblages in Northwest Pangea: A case for a shallow-marine habitable zone. *Geology* **36**, 771–774 (2008).
81. L. A. Buatois, M. G. Mángano, The déjà vu effect: Recurrent patterns in exploitation of ecospace, establishment of the mixed layer, and distribution of matgrounds. *Geology* **39**, 1163–1166 (2011).
82. T. J. Thomson, M. L. Droser, Swimming reptiles make their mark in the Early Triassic: Delayed ecologic recovery increased the preservation potential of vertebrate swim tracks. *Geology* **43**, 215–218 (2015).
83. S. Pruss, M. Fraiser, D. J. Bottjer, Proliferation of Early Triassic wrinkle structures: Implications for environmental stress following the end-Permian mass extinction. *Geology* **32**, 461–464 (2004).
84. C. G. Barras, R. J. Twitchett, Response of the marine infauna to Triassic-Jurassic environmental change: Ichnological data from southern England. *Palaeogeogr. Palaeoclimatol. Palaeoecol.* **244**, 223–241 (2007).

85. R. Hofmann, B. Gutwasser, H. Hüneke, D. Korn, Firm evidence for a post-extinction ichnofauna: Earliest Carboniferous *Cruziana reticulata* assemblage from the Anti-Atlas of Morocco. *Lethaia* **53**, 118–128 (2020).
86. M. L. Droser, D. J. Bottjer, "Trace fossils and ichnofabric in Leg 119 cores," in *Proceedings of the Ocean Drilling Program, Scientific Results*, J. Barron, Larsen, B., Eds. (1991), Ocean Drilling Program, vol. 119, pp. 635–641.
87. A. A. Ekdale, R. G. Bromley, Sedimentology and ichnology of the Cretaceous-Tertiary boundary in Denmark: Implications for the causes of the terminal Cretaceous extinction. *J. Sediment. Petrol.* **54**, 681–703 (1984).
88. C. E. Savrda, J. V. Browning, H. Krawinkel, S. P. Hesselbo, Firmground ichnofabrics in deep-water sequence stratigraphy, Tertiary clinoform-toe Deposits, New Jersey Slope. *Palaios* **16**, 294–305 (2001).
89. L. G. Herringshaw, N. S. Davies, Bioturbation levels during the end-Ordovician extinction event: A case study of shallow marine strata from the Welsh Basin. *Aquat. Biol.* **2**, 279–287 (2008).
90. P. B. Wignall, R. Morante, R. Newton, The Permo-Triassic transition in Spitsbergen: $\delta^{13}C_{org}$ chemostratigraphy, Fe and S geochemistry, facies, fauna and trace fossils. *Geol. Mag.* **135**, 47–62 (1998).
91. J. C. Zachos, D. Kroon, P. Blum, "Site 1262," in *Proceedings of the Ocean Drilling Program, Initial Reports*, J. C. Zachos, D. Kroon, P. Blum, J. Bowles, P. Gaillot, T. Hasegawa, E. C. Hathorne, D. A. Hodell, D. C. Kelly, J.-H. Jung, S. M. Keller, Y. S. Lee, D. C. Leuschner, L. Zhifei, K. C. Lohmann, L. Lourens, S. Monechi, M. J. Nicolo, I. Raffi, C. Riesselman, U. Röhl, S. A. Schellenberg, D. Schmidt, A. Sluijs, D. J. Thomas, E. Thomas, H. Vallius, H. Neville, K. Sherar, Eds. (Texas A&M University, 2004), pp. 1–92.
92. T. J. Bralower, D. C. Kelly, S. Gibbs, K. Farley, L. Eccles, T. L. Lindemann, G. J. Smith, Impact of dissolution on the sedimentary record of the Paleocene-Eocene thermal maximum. *Earth Planet. Sci. Lett.* **401**, 70–82 (2014).
93. M. Zill, "Deep sea sediment alteration across the Paleocene-Eocene Thermal Maximum," thesis, University of California, Riverside, Riverside, CA (2022).
94. D. J. Bottjer, M. L. Droser, D. Jablonski, "Bathymetric trends in the history of trace fossils," in *New Concepts in the Use of Biogenic Sedimentary Structures for Paleoenvironmental Interpretation*, D. J. Bottjer, Ed. (Pacific Section SEPM, 1987), pp. 57–65.
95. D. Jablonski, D. J. Bottjer, "Onshore-offshore trends in marine invertebrate evolution," in *Causes of Evolution: A Paleontological Perspective*, R. M. Ross, W. D. Allmon, Eds. (University of Chicago Press, 1990), pp. 21–75.
96. T. P. Crimes, M. A. Fedonkin, Evolution and dispersal of deepsea traces. *Palaios* **9**, 74–83 (1994).
97. E. A. Sperling, T. H. Boag, M. I. Duncan, C. R. Endriga, J. A. Marquez, D. B. Mills, P. M. Monarrez, J. A. Sclafani, R. G. Stockey, J. L. Payne, Breathless through time: Oxygen and animals across Earth's history. *Biol. Bull.* **243**, 184–206 (2022).
98. A. T. Cribb, S. J. van de Velde, W. M. Berelson, D. J. Bottjer, F. A. Corsetti, Ediacaran–Cambrian bioturbation did not extensively oxygenate sediments in shallow marine ecosystems. *Geobiology* **21**, 435–453 (2023).
99. K. Hantsoo, M. Gomes, D. Brenner, J. Cornwell, C. M. Palinkas, S. Malkin, Trends in estuarine pyrite formation point to an alternative model for Paleozoic pyrite burial. *Geochim. Cosmochim. Acta* **374**, 51–71 (2024).
100. L. G. Tarhan, M. Zhao, N. J. Planavsky, Bioturbation feedbacks on the phosphorus cycle. *Earth Planet. Sci. Lett.* **566**, 116961 (2021).
101. A. W. Dale, R. A. Boyle, T. M. Lenton, E. D. Ingall, K. Wallmann, A model for microbial phosphorus cycling in bioturbated marine sediments: Significance for phosphorus burial in the early Paleozoic. *Geochim. Cosmochim. Acta* **189**, 251–268 (2016).
102. M. W. Wallace, A. V. S. Hood, A. Shuster, A. Greig, N. J. Planavsky, C. P. Reed, Oxygenation history of the Neoproterozoic to early Phanerozoic and the rise of land plants. *Earth Planet. Sci. Lett.* **466**, 12–19 (2017).
103. E. Kristensen, G. Penha-Lopes, M. Delefosse, T. Valdemarsen, C. O. Quintana, G. T. Banta, What is bioturbation? The need for a precise definition for fauna in aquatic sciences. *Mar. Ecol. Prog. Ser.* **446**, 285–302 (2012).
104. N. Volkenborn, L. Polerecky, S. I. C. Hedtkamp, J. E. E. van Beusekom, D. de Beer, Bioturbation and bioirrigation extend the open exchange regions in permeable sediments. *Limnol. Oceanogr.* **52**, 1898–1909 (2007).
105. R. C. Aller, Bioturbation and remineralization of sedimentary organic matter: Effects of redox oscillation. *Chem. Geol.* **114**, 331–345 (1994).
106. R. A. Berner, D. E. Canfield, A new model for atmospheric oxygen over Phanerozoic time. *Am. J. Sci.* **289**, 333–361 (1989).
107. S. van de Velde, F. J. R. Meysman, The influence of bioturbation on iron and sulphur cycling in marine sediments: A model analysis. *Aquat. Geochem.* **22**, 469–504 (2016).
108. V. P. Wright, L. Cherns, Leaving no stone unturned: The feedback between increased biotic diversity and early diagenesis during the Ordovician. *J. Geol. Soc. London* **173**, 241–244 (2016).
109. A. A. Ekdale, J. M. de Gibert, Paleoethologic significance of bioglyphs: Fingerprints of the subterraneans. *Palaios* **25**, 540–545 (2010).
110. R. G. Bromley, A. A. Ekdale, Composite ichnofabrics and tiering of burrows. *Geol. Mag.* **123**, 59–65 (1986).
111. R. K. Goldhammer, Compaction and decompaction algorithms for sedimentary carbonates. *J. Sediment. Res.* **67**, 26–35 (1997).
112. H. Hillgärtner, A. Strasser, Quantification of high-frequency sea-level fluctuations in shallow-water carbonates: An example from the Berriasian-Valanginian (French Jura). *Palaeogeogr. Palaeoclimatol. Palaeoecol.* **200**, 43–63 (2003).
113. Ø. Hammer, D. A. T. Harper, P. D. Ryan, PAST: Paleontological statistics software package for education and data analysis. *Palaeontol. Electronica* **4**, 9 (2001).
114. W. Gearty, deeptime: An R package that facilitates highly customizable visualizations of data over geological time intervals. EarthArXiv, 10.31223/X5841N (2024).
115. L. J. Zhang, Y. A. Qi, L. A. Buatois, M. G. Mangano, Y. Meng, D. Li, The impact of deep-tier burrow systems in sediment mixing and ecosystem engineering in early Cambrian carbonate settings. *Sci. Rep.* **7**, 45773 (2017).
116. P. M. Myrow, *Thalassinoides* and the enigma of early Paleozoic open-framework burrow systems. *Palaios* **10**, 58–74 (1995).
117. T. Oji, S. Q. Dornbos, K. Yada, H. Hasegawa, S. Gonchigdorj, T. Mochizuki, H. Takayanagi, Y. Iryu, Penetrative trace fossils from the late Ediacaran of Mongolia: Early onset of the agronomic revolution. *R. Soc. Open Sci.* **5**, 172250 (2018).
118. E. F. Smith, F. A. Macdonald, T. A. Petach, U. Bold, D. P. Schrag, Integrated stratigraphic, geochemical, and paleontological late Ediacaran to early Cambrian records from southwestern Mongolia. *Geol. Soc. Am. Bull.* **128**, 442–468 (2016).
119. M. K. Gingras, S. G. Pemberton, T. Saunders, Bathymetry, sediment texture, and substrate cohesiveness; their impact on modern *Glossifungites* trace assemblages at Willapa Bay, Washington. *Palaeogeogr. Palaeoclimatol. Palaeoecol.* **169**, 1–21 (2001).
120. M. K. Gingras, J. A. Maceachern, R. K. Pickerill, Modern perspectives on the *Teredolites* ichnofacies: Observations from Willapa Bay, Washington. *Palaios* **19**, 79–88 (2004).
121. A. K. Rindsberg, D. C. Kopaska-Merkel, "*Treptichnus* and *Arenicolites* from the Steven C. Minkin Paleozoic Footprint Site (Langsettian, Alabama, USA)," in *Pennsylvanian Footprints in the Black Warrior Basin of Alabama*, A. K. Rindsberg, D. C. Kopaska-Merkel, Eds. (Alabama Paleontological Society Monograph, 2005), pp. 121–141.
122. C. K. Chamberlain, J. L. Baer, *Ophiomorpha* and a new thallassinid burrow from the Permian of Utah. *Brigham Young Univ. Geol. Studies.* **20**, 79–94 (1973).
123. L.-J. Zhang, R.-Y. Fan, Y.-M., *Zoophycos* macroevolution since 541 Ma. *Sci. Rep.* **5**, 14954 (2015).
124. M. L. Droser, "Trends in extent and depth of bioturbation in Great Basin Precambrian–Ordovician strata, California, Nevada and Utah," thesis, University of Southern California (1987).
125. L. G. Tarhan, M. L. Droser, N. C. Hughes, Exceptional trace fossil preservation and mixed layer development in Cambro-Ordovician siliciclastic strata. *Mem. Assoc. Australas. Palaeontol.* **45**, 71–88 (2014).
126. R. Mikuláš, T. Lehotsky, O. Bábek, Lower Carboniferous ichnofabrics of the Culm facies: A case study of the Moravice Formation (Moravia and Silesia, Czech Republic). *Geol. Carpath.* **53**, 141–148 (2002).
127. P. J. Orr, M. J. Benton, N. H. Trewin, Deep marine trace fossil assemblages from the Lower Carboniferous of Menorca, Balearic Islands, western Mediterranean. *Geol. J.* **31**, 235–258 (1996).
128. D. J. Bottjer, M. L. Droser, Ichnofabric and basin analysis. *Palaios* **6**, 199–205 (1991).
129. L. A. Buatois, M. G. Mángano, N. J. Minter, K. Zhou, M. Wisshak, M. A. Wilson, R. A. Olea, Quantifying ecospace utilization and ecosystem engineering during the early Phanerozoic—The role of bioturbation and bioerosion. *Sci. Adv.* **6**, eabb0618 (2020).
130. L. A. Buatois, M. G. Mángano, M. Paz, N. J. Minter, K. Zhou, Early colonization of the deep-sea bottom—The protracted build-up of an ecosystem. *Proc. Natl. Acad. Sci. U.S.A.* **122**, e2414752122 (2025).
131. A. Uchman, "Phanerozoic history of deep-sea trace fossils," in *The Application of Ichnology to Palaeoenvironmental and Stratigraphic Analysis*, D. McIlroy, Ed. (The Geological Society of London, 2004), pp. 125–139.
132. G. Pieńkowski, A. Uchman, K. Ninard, S. P. Hesselbo, Ichnology, sedimentology, and orbital cycles in the hemipelagic Early Jurassic Laurasian Seaway (Pliensbachian, Cardigan Bay Basin, UK). *Glob. Planet. Change* **207**, 103648 (2021).
133. R. K. Pickerill, P. F. Williams, Deep burrowing in the early Palaeozoic deep sea: Examples from the Cambrian(?)–Early Ordovician Meguma Group of Nova Scotia. *Can. J. Earth Sci.* **26**, 1061–1068 (1989).
134. D. Olivero, Early Jurassic to Late Cretaceous evolution of *Zoophycos* in the French Subalpine Basin (southeastern France). *Palaeogeography, Palaeoclimatology, Palaeoecology* **192**, 59–78 (2003).
135. H. O. Pörtner, R. Knust, Climate change affects marine fishes through the oxygen limitation of thermal tolerance. *Science* **315**, 95–97 (2007).
136. J. L. Penn, C. Deutsch, J. L. Payne, E. A. Sperling, Temperature-dependent hypoxia explains biogeography and severity of end-Permian marine mass extinction. *Science* **362**, eaat1327 (2018).
137. D. Ouellette, G. Desrosiers, J. P. Gagne, F. Gilbert, J. C. Poggiale, P. U. Blier, G. Stora, Effects of temperature on *in vitro* sediment reworking processes by a gallery biodiffusor, the polychaete *Neanthes virens*. *Mar. Ecol. Prog. Ser.* **266**, 185–193 (2004).

138. G. Bernard, M. L. Delgard, O. Maire, A. Ciutat, P. Lecroart, B. Deflandre, J. C. Duchêne, A. Grémare, Comparative study of sediment particle mixing in a *Zostera noltei* meadow and a bare sediment mudflat. *Mar. Ecol. Prog. Ser.* **514**, 71–86 (2014).
139. L. Pascal, O. Maire, B. Deflandre, A. Romero-Ramirez, A. Grémare, Linking behaviours, sediment reworking, bioirrigation and oxygen dynamics in a soft-bottom ecosystem engineer: The mud shrimp *Upogebia pusilla* (Petagna 1792). *J. Exp. Mar. Biol. Ecol.* **516**, 67–78 (2019).
140. T. S. Bianchi, C. J. Brown, P. V. R. Snelgrove, R. R. E. Stanley, D. Cote, C. Morris, Benthic invertebrates on the move: A tale of ocean warming and sediment carbon storage. *Limnol. Oceanogr. Bull.* **32**, 1–5 (2023).
141. P. D. Wall, L. C. Ivany, B. H. Wilkinson, Revisiting Raup: Exploring the influence of outcrop area on diversity in light of modern sample-standardization techniques. *Paleobiology* **35**, 146–167 (2009).

Acknowledgments: We thank A. Ridgwell and other members of the iMUDS working group for critical discussion that helped to shape the framework of this manuscript. We also thank C. Savrda for use of the images shown in Fig. 1 (I and J), B. Beaty for use of the image shown in Fig. 1K, and A. Ahmad-Rizal and the Division of Invertebrate Paleontology of the Yale Peabody Museum for the image shown in Fig. 2F. We thank the four reviewers for comments that improved this manuscript. **Funding:** This research was supported by Yale University (L.G.T.) and a National Science Foundation Graduate Research Fellowship (K.H.P.). **Author contributions:** Conceptualization: M.E.C., L.G.T., D.J.B., and M.L.D. Methodology: L.G.T., M.E.C., D.J.B., and K.H.P. Investigation: L.G.T., K.H.P., M.E.C., M.Z., A.T.C., and W.P. Validation: L.G.T. Data curation: L.G.T. and M.E.C. Visualization: L.G.T. and K.H.P. Supervision: L.G.T., D.J.B., and M.L.D. Writing—original draft: L.G.T., K.H.P., M.Z., and D.J.B. Writing—review and editing: L.G.T., K.H.P., D.J.B., and M.E.C. Project administration: L.G.T. Resources: L.G.T. Funding acquisition: L.G.T. **Competing interests:** The authors declare that they have no competing interests. **Data and materials availability:** All data needed to evaluate the conclusions in the paper are present in the paper and/or the Supplementary Materials.

Submitted 20 November 2024
Accepted 2 July 2025
Published 30 July 2025
10.1126/sciadv.adu7719